JPhys Energy

PAPER • OPEN ACCESS

A review of chemical looping reforming technologies for hydrogen production: recent advances and future challenges

To cite this article: Rouzbeh Ramezani *et al* 2023 *J. Phys. Energy* **5** 024010

IOP Publishing J. Phys. Energy 5 (2023) 024010 https://doi.org/10.1088/2515-7655/acc4e8

Journal of Physics: Energy

RECEIVED
11 September 2022

REVISED
7 March 2023

ACCEPTED FOR PUBLICATION
16 March 2023

PUBLISHED
27 March 2023

PAPER

A review of chemical looping reforming technologies for hydrogen production: recent advances and future challenges

Rouzbeh Ramezani, Luca Di Felice and Fausto Gallucci*

Sustainable Process Engineering, Department of Chemical Engineering and Chemistry, Eindhoven University of Technology, De Rondom 70, 5612 AP Eindhoven, The Netherlands

* Author to whom any correspondence should be addressed.

E-mail: f.gallucci@tue.nl

Keywords: CO_2 capture, chemical looping, hydrogen production, oxygen carrier, clean energy

Abstract

Faced with increasingly serious energy and global warming, it is critical to put forward an alternative non-carbonaceous fuel. In this regard, hydrogen appears as the ultimate clean fuel for power and heat generation, and as an important feedstock for various chemical and petrochemical industries. The chemical looping reforming (CLR) concept, is an emerging technique for the conversion of hydrocarbon fuels into high-quality hydrogen via the circulation of oxygen carriers which allows a decrease in CO_2 emissions. In this review, a comprehensive evaluation and recent progress in glycerol, ethanol and methane reforming for hydrogen production are presented. The key elements for a successful CLR process are studied and the technical challenges to achieve high-purity hydrogen along with the possible solutions are also assessed. As product quality, cost and the overall efficiency of the process can be influenced by the oxygen carrier materials used, noteworthy attention is given to the most recent development in this field. The use of Ni, Fe, Cu, Ce, Mn and Co-based material as potential oxygen carriers under different experimental conditions for hydrogen generation from different feedstock by CLR is discussed. Furthermore, the recent research conducted on the sorption-enhanced reforming process is reviewed and the performance of the various type of CO_2 sorbents such as CaO, Li_2ZrO_3 and MgO is highlighted.

1. Introduction

Nowadays, the production of clean energy and the reduction of greenhouse gas emissions have drawn much attention all over the world (Teh *et al* 2021). In the past few decades, fossil fuels such as petroleum and coal have become the main energy sources that lead to the exponential growth of the CO_2 concentration in the atmosphere from 310 ppm in 1960–419 ppm in 2021, resulting in significant environmental concerns (Alam *et al* 2020). The rise of global temperature, species extinction, sea-level rise, and ocean acidification are some examples of the consequences of anthropogenic greenhouse gases emission into the atmosphere (Hu *et al* 2016). Therefore, it is both imperative and critical to develop efficient strategies along with greater reliance on renewable energy to reduce global CO_2 emissions.

The utilization of hydrogen as an alternative to carbon-containing fossil fuels indicates an additional approach to mitigate global warming risks (Wassie *et al* 2017). Thanks to its pollution-free characteristics as well as its high heating value and rich resources, hydrogen has great potential to become a promising substitute as a clean energy carrier (van Renssen 2020). On the other hand, hydrogen demand is expected to continually increase with increasing industrialization over time and the world population (Chaubey *et al* 2013).

Although carbon-based fuels supply 85% of the world's energy claim, it is predicted that hydrogen would be responsible for 90% of the world's energy in 2080 which shows its significant role in future energy (Roslan *et al* 2020). The food industry, treating metals, chemical manufacturing industry, petroleum refining, glass purification, hydrocracking and fuel cells are the main sectors for hydrogen application (Barreto *et al* 2003, Delparish and Avci 2016). In order to accept hydrogen as a major energy source, it should be produced sustainably and efficiently. Hydrogen is classified into three main classes including blue hydrogen, grey hydrogen and green hydrogen depending on their production approach and raw materials (Atilhan *et al* 2021).

Green hydrogen has a much lower environmental cost compared to grey and blue-based technologies (Baykara 2018). In recent years, great effort has been put into advancement in materials, cost and technical issues during producing green hydrogen from renewables that will reduce the cost of production of green hydrogen by up to 70% during the next decade (Atilhan *et al* 2021).

The production of hydrogen can be done using various technologies such as biological processes, photoelectrolysis, water splitting by high-temperature heat, water electrolysis, gasification of coal and biomass, natural gas, or biogas reforming (Iriondo *et al* 2008). Several factors such as system integration options, technological availability, resources and their use, costs, efficiency and environmental impacts should take into account in order to select a hydrogen production method (Ji and Wang 2021). Among them, chemical looping techniques are the most promising and innovative platform for hydrogen production and CO_2 capture (Wang *et al* 2015). Chemical-looping refers to a cycling process that utilizes a solid metal oxide to transfer oxygen from the air to the fuel via redox reactions (Lee *et al* 2021). From an energy point of view, chemical looping is a unique approach that can not only convert different feedstocks to various value-added chemicals such as alkene, ammonia, synthesis gas and H_2/CO with low production cost but also tackle the issue of CO_2 capture (Fan *et al* 2015).

Depending on gas product components and the differences in oxygen originations, this technology can be employed in a wide range of applications such as chemical looping hydrogen generation, chemical looping reforming (CLR), chemical looping gasification and chemical looping combustion (Osman *et al* 2021). The keys to a successful implementation of a chemical looping technique are an appropriate selection of oxygen carriers and an effective reactor design which directed the attempts toward the development of oxygen carriers (Fan *et al* 2012). Throughout the years, a range of chemical looping technology in different applications have been reviewed by researchers in the literature which mainly focused on the advances of oxygen carriers in an application or CLR based on a specific feedstock. CLR concept involves oxidation of a fuel via cyclic reduction and oxidation of a solid oxygen carrier. The main advantage of this process is that the heat needed for converting fuel to hydrogen is supplied without costly oxygen production, without mixing of air with carbon containing fuel gases or without using part of the hydrogen generated in the system (de Diego *et al* 2009). The heat for the endothermic reduction reactions in fuel reactor is provided by the circulating solids coming from the air reactor at higher temperature meaning no external heat is required.

Another specific advantage of the a-CLR process is the possibility of obtaining pure N_2 at the outlet stream of the air reactor by controlling the amount of air fed into the air reactor (García-Díez *et al* 2017). There is less concern with respect to coke formation in CLR because cycles are self-regenerative. However, deactivation can still pose limitations in many oxide systems because of incomplete coke removal (Sastre *et al* 2019). Circulating fluidized beds in CLR provides good contact between gas and solids and allows a smooth flow of oxygen-carrier particles between the reactors. One of the key issues regarding system performance in CLR technology development is the selection of oxygen carrier. The carbon deposition of oxygen carriers can cause poor stability which is still a serious challenge in industrial application. Moreover, material deactivation caused by carbon deposition is also one of the main issues. Toxicity and the cost of oxygen carriers may also limit their application (Meshksar *et al* 2017).

Table 1 summarizes an overview of studies that have recently been published in the literature in the field of chemical looping. Masoudi Soltani *et al* (2021) reviewed the recent developments in hydrogen production by sorption-enhanced steam methane reforming (SE-SMR). The authors presented a discussion on the advancements in catalysts/adsorbents preparation and process optimization. Roslan *et al* (2020) highlighted the recent advances in Ni-based glycerol reforming processes. They discussed the role of nickel as a catalyst in the reforming reactions and the challenges faced by this technology. A brief review of recent findings in the development of oxygen carrier materials for chemical looping was carried out by Cheng *et al* (2018). Tang *et al* (2015) provided a review of the recent advances in oxygen carriers utilized in the chemical-looping reforming of methane. According to reported studies in the literature, it seems that a review paper that comprehensively focuses on the CLR system from different feedstocks with an extensive review of oxygen carrier materials and CO_2 sorbents is still missing.

Therefore, in this work, the authors reviewed key technological breakthroughs in the field of CLR from a different point of view to provide a comprehensive assessment. The review starts with recent findings on CLR based on methane, ethanol and glycerol, followed by their performance and advantages. Major efforts have been made toward main achievements in the characterization and preparation of the most used oxygen carrier materials. Next, the importance of the selection of different CO_2 sorbents was assessed and their results and progress were presented. Finally, the important challenges related to CLR systems for high-purity hydrogen production were highlighted.

Table 1. List of published review works done on chemical looping technologies.

References	Review description
Masoudi Soltani *et al* (2021)	Recent development in hydrogen production via steam methane reforming
Roslan *et al* (2020)	Recent findings on Ni-based glycerol reforming processes
Cheng *et al* (2018)	A brief overview of development of oxygen carriers for chemical looping systems
Tang *et al* (2015)	A review of oxygen carriers for methane-based chemical looping reforming

2. CLR

In recent years, various sources such as coal, natural gas and biomass have been considered for CLR technologies. While many feedstocks can be utilized for reforming, methane is preferred for hydrogen production as it has low cost, high availability, high hydrogen-to-carbon ratio and lower byproduct formation in comparison to other starting materials (Alirezaei *et al* 2018). Steam methane reforming is currently the most common and developed technology used for hydrogen production at large scales (García-Labiano *et al* 2015a). Although the main experience of obtaining hydrogen by the CLR process is with gaseous fuels, liquid fuels from renewable sources (biomass or biofuels) are becoming more relevant in the last years for reasons of sustainability. Among them, ethanol offers high possibilities due to the large amount available. High hydrogen content, less hazard, safe transport and high heating value are advantages that make ethanol an important candidate for hydrogen production (Vizcaíno *et al* 2008). Besides ethanol, other bio-source has been proved to be a good feedstock for steam reforming such as glycerol. The selection of glycerol feedstock is based in part on its ready and cheap availability as a by-product of bio-diesel production (Ni *et al* 2017).

All hydrocarbon fuels can be used as raw material in the production of hydrogen. CLR can be operated with both liquid and gaseous fuels. The design of fuel-reactor and the type of oxygen carrier strongly depend on fuel type and feed phase. The fluidized bed, moving bed and packed bed reactors were studied in the literature for CLR for liquid, and gaseous fuels (Vos *et al* 2020). The production cost and the purity of produced hydrogen, heat transfer and process control are also important factors in selection of fuel. Reactions and the operating conditions in fuel reactors such as fuel-to-water ratio, pressure, temperature and contact time vary with feed composition. For example, steam reforming of glycerol involves complex reactions that result in several intermediates affecting the selectivity of the hydrogen. The heats of the reaction depend on the fuel type and the metal oxide used as an oxygen carrier. Both gaseous and liquid fuels in CLR may contain impurities that limit the oxygen transfer capacity, reactivity, and selectivity. To achieve a full conversion of fuel and a long lifetime of the oxygen carrier, it is crucial to select the oxygen carrier depending on the fuel used in the fuel reactor (Porrazzo *et al* 2014). A summary of studies performed on CLR using different fuels was listed in table 2.

2.1. CLR of methane

Methane is the main component of natural gas and unconventional gas, and methane reforming is a high-efficiency and low-energy approach to methane utilization to satisfy the global demand for energy (Yin *et al* 2022). The CLR is similar to chemical looping combustion, but instead of full combustion of methane to generate water, CO_2 and heat, the methane is partially oxidized by an oxygen carrier to prepare high-quality syngas, which is suitable for high-value-added downstream chemical products (Adanez *et al* 2012). Therefore, the concept of CLR targets the production of $H_2 + CO$ by partially oxidizing methane in the fuel reactor by the lattice oxygen of a solid oxygen carrier while the oxygen-depleted material is re-oxidized in an air reactor (Sun *et al* 2022). The heat generated from the redox reactions is used for the endothermic steam/dry reforming (DRM) of methane to produce $H_2 + CO$ (Argyris *et al* 2022). The CLR consists of two reactors, most commonly fixed beds, moving beds and fluidized beds. To choose the right reactor configuration, several factors such as target heat/mass transfer rates, reaction kinetics, and the desired extent of reduction of the oxygen carriers should be considered (Sun *et al* 2020). Depending on the ratio of oxygen to fuel and the nature of the oxygen carrier, the following reactions can occur during a methane reforming process that can affect the reactor design and syngas selectivity targets (Sun *et al* 2020).

Partial methane oxidation:

$$CH_4 + Me_xO_y \rightarrow 2H_2 + CO + Me_xO_{y-1}. \tag{R-1}$$

Full methane oxidation:

$$CH_4 + 4Me_xO_y \rightarrow 2H_2O + CO_2 + 4Me_xO_{y-1}. \tag{R-2}$$

Table 2. Summary of chemical looping reforming of various feedstocks studied in the literature.

Oxygen carrier	Reactant	Temperature (°C)	H_2 Purity	Reactant conversion	References
CuO–Ni/Al_2O_3	Ethanol	500–650	83%	98%–100%	Nimmas *et al* (2020)
NiO/Al_2O_3	Ethanol	600	97%	82%–93%	Dou *et al* (2018)
NiFe/MgAl	Ethanol	400–700	78%	100%	Saupsor *et al* (2021)
Ni/Al_2O_4	Ethanol	900	82%	91%	Zhang *et al* (2021a)
Ni/Al_2O_3	Ethanol	600–900	61%	72%	Wang *et al* (2016b)
NiO–CuO/Al_2O_3	Ethanol	100–900	N.A.	N.A.	López Ortiz *et al* (2015)
LaSrNiO	Ethanol	650	75%–83%	80%–85%	Zhang *et al* (2017)
CeNi/SBA	Ethanol	200–900	90%–95%	100%	Wang *et al* (2016a)
$NiFe_2O_4$	Ethanol	450	70%–80%	100%	Trevisanut *et al* (2015)
Ni/CeO_2	Ethanol	200–800	N.A.	88%	Isarapakdeetham *et al* (2020)
$NiMn_2O_4$	Ethanol	500–800	N.A.	N.A.	Wang *et al* (2017)
$LaNiO_3$/MMT	Ethanol	650	70%–80%	87%	Li *et al* (2017)
Ni/CeO_2	Ethanol	100–600	88%	80%	Li *et al* (2018b)
NiO/Al_2O_3	Ethanol	850–950	62%	100%	García-Labiano *et al* (2015a)
NiO/MMT	Ethanol	550	60%–70%	70%–80%	Jiang *et al* (2016)
Ir/La_2O_3	Ethanol	400–850	90%–100%	N.A.	Yang *et al* (2011)
Ni–Ca/Al_2O_3	Ethanol	550–650	N.A.	99%	Elias *et al* (2013)
Ce–Ni/Fe	Glycerol	200–800	80%–90%	60%–80%	Luo *et al* (2022)
CeNiO	Glycerol	500–650	85%	60%	Wang *et al* (2016a)
Rh/Al_2O_3	Glycerol	550–700	N.A.	93%–100%	Delparish *et al* (2019)
NiO	Glycerol	750–850	60%	100%	Adánez-Rubio *et al* (2021)
Fe–Ce–Ni	Glycerol	600–800	80.6%	70%–100%	Lu *et al* (2021)
Rh/UGSO	Glycerol	650	N.A.	94%–100%	Sahraei *et al* (2021)
Ni–Mg/ATP	Glycerol	400–800	94.7%	87.9%	Qingli *et al* (2021)
Ni/Al_2O_3	Glycerol	600–750	N.A.	65%–95%	Tavanarad *et al* (2021)
Ni/ZrO_2	Glycerol	650	94%	99%	Jiang *et al* (2018b)
Rh–Mg/Al_2O_4	Glycerol	300–600	76%	99.6%	Senseni *et al* (2017)
Ni–Co–Cu/Al_2O_3	Glycerol	400–750	65%	80%–95%	Papageridis *et al* (2016)
Ce–Ni/PSNT	Glycerol	650	70%–90%	88%	Jiang *et al* (2018a)
Ni/Al_2O_3	Glycerol	500–600	80%–95%	N.A.	Dou *et al* (2014)
Ni/Al_2O_3	Glycerol	550	87.9%	85%–98%	Ni *et al* (2017)
Ni/Al_2O_3	Glycerol	450–600	93%	99%	Jiang *et al* (2015)
N.A.	Glycerol	350–700	45%–55%	90%–96%	Chen *et al* (2011)
Rh–CeO_2/Al_2O_3	Glycerol	400–750	78%	90%	Charisiou *et al* (2020)
Ni/Al_2O_3	Glycerol	450–650	N.A.	100%	Wu *et al* (2013)
Ni–Cu–Al	Glycerol	450–650	92.9	90.9%	Wang *et al* (2013)
Ni/Al_2O_3	Glycerol	400–700	97%	100%	Dou *et al* (2009)
Ni/Al_2O_3	Glycerol	600–700	65%	50%	Jiang *et al* (2020)
$LaSrFeO_3$	Methane	850	N.A.	85%–88%	Sastre *et al* (2022)
LaSrMnCoO	Methane	850	65%	40%–78%	Yin *et al* (2022)
$CeFeO_3$	Methane	650–850	80%–85%	70%–80%	Zhang *et al* (2020)
Fe_2O_3/$MgAl_2O_4$	Methane	900	91%–100%	83%–92%	Hu *et al* (2021a)
NiO/$CeZrO_4$	Methane	700	N.A.	52.8%	Zhang *et al* (2021b)
Ni/Fe	Methane	800	93%	96%	Hu *et al* (2021c)
Ni–CeO2/MgO	Methane	550–700	N.A.	45%	Khajenoori *et al* (2015)
Ni–Cu	Methane	800	70%–80%	30%	Huang *et al* (2019)
NiO	Methane	650	75%–80%	80%–87%	Antzara *et al* (2016)
Ni–CeO2/Al2O3	Methane	700	N.A.	95%	Shamskar *et al* (2017)
Ni/CeO2-IMP	Methane	800	N.A.	90%	Guerrero-Caballero *et al* (2019)
Cu–Ni–Mn	Methane	650	N.A.	99.4%	Nazari *et al* (2021)
$LaFe_2O_3$/Al_2O_3	Methane	800–900	N.A.	55%	Dai *et al* (2012)
Fe_2O_3/Al_2O_3	Methane	700–900	96%	98%	Zhu *et al* (2019)
$LaSrFeO_6$	Methane	500–900	50%–60%	70%–85%	Zhao *et al* (2019)
$Ce_{0.5}Fe_{0.5}O_2$	Methane	800–900	92%	90%–98%	Zhu *et al* (2013)
$LaFe_{0.7}Co_{0.3}O_3$	Methane	500–700	50%	85%	Zhao *et al* (2016)
Fe/Al_2O_3	Methane	600–800	55%	99%	Spallina *et al* (2016a)
NiO	Methane	600–900	$>$50%	92%	Spallina *et al* (2017)
NiO/$CaAl_2O_3$	Methane	400–900	N.A.	99%	Argyris *et al* (2022)
17%Ni/Al_2O_3	Methane	600–750	60%	40%	Martini *et al* (2021a)
NiO	Methane	450–650	N.A.	90%	Medrano *et al* (2018)
Ni–Ce	Methane	600–800	N.A.	50%–61%	Iglesias *et al* (2017)

Methane decomposition:

$$CH_4 \rightarrow C + 2H_2. \tag{R-3}$$

Water-gas shift:

$$CO + H_2O \rightarrow CO_2 + H_2. \tag{R-4}$$

Steam methane reforming:

$$CH_4 + H_2O \rightarrow CO + 3H_2. \tag{R-5}$$

Dry methane reforming:

$$CH_4 + CO_2 \rightarrow 2CO + 2H_2. \tag{R-6}$$

From a product selectivity point of view, various products can appear in methane reduction according to the above equations. Although Fe-based materials are attractive oxygen carriers due to environmental compatibility, low cost, and thermodynamic advantages, pure iron oxides cannot meet the requirements of methane reforming in terms of methane conversion and hydrogen selectivity (Neal *et al* 2015). Therefore, Fe-based materials need to be deeply reduced to FeO/Fe to produce hydrogen. Furthermore, as the reactivity of Fe to methane is low compared with other transition metals (Guerrero-Caballero *et al* 2019), many researchers have studied adding promoters to enhance the reactivity to methane. In comparison to Fe-based materials with 84% methane conversion, Fe–Ni, Fe–Co and Fe–Cu showed respectively 92%, 83% and 85% methane conversion in CLR of methane at 900 °C, indicating methane decomposition rather than methane oxidation with lattice oxygen led to high methane conversion. It was shown that the promoters have a positive effect on the hydrogen purity of iron oxygen carriers. The hydrogen purity of methane reforming after ten cycles was reported 91%, 94%, 98% and 100% for Fe, Fe–Ni, Fe–Cu and Fe–Co, respectively. Co can increase the amount of active lattice oxygen instead of the activity of lattice oxygen, and Cu can activate the initial reduction but restrain the deep reduction of Fe-based oxygen carriers. The strongest interaction with Fe was observed in Ni-promoted oxygen carriers and a small amount of addition can increase the extend of deep reduction. Therefore, the addition of Ni, Co and Cu to Fe-based oxygen carriers can offer the higher H_2 purity and (H_2–CO) yield but a lower CO purity due to enhanced ability to oxygen diffusion (Hu *et al* 2021a).

Compared to the methane steam reforming reaction, the reaction rate in partial oxidation of methane (POM) was reported to be hundreds of times higher. Furthermore, it has been reported that reaction performance in methane reforming unit is relatively sensitive to temperature changes in a temperature range of 500 °C–700 °C (Zhang *et al* 2021b). Qin *et al* (2018) proved that the addition of 1% of Cu dopant to Fe-based oxygen carriers leads to a higher reactivity at low temperatures. Based on their funding, the methane conversion rate in Cu–Fe_2O_3 is 470% higher than that Fe_2O_3 at 700 °C which results in a decrease in energy consumption by up to 35%.

Detailed study of the effect of steam flow to oxygen carrier ratio and methane flow to oxygen carrier ratio on methane conversion and product yield in steam methane reforming was performed by several researchers (Hu *et al* 2021c). It was reported that hydrogen concentration decreases when steam flow to oxygen carrier ratio increases while CO_2 and CO concentrations increased. This can be explained by the fact that that CH_4 complete oxidation reaction is limited under the condition of high steam concentration, which leads to the oxidation of CH_4 into CO_2 and H_2 and the conversion of CH_4 into carbon and H_2. The CO_2 generated in the reaction process is absorbed by CaO to produce $CaCO_3$. When steam to oxygen carrier ratio increases, the CO_2 concentration increases slightly. Moreover, the excessive steam promotes the oxidation of carbon to produce CO. Therefore, the H_2 concentration decreases and the concentration of CH_4 and CO increases with the increase of steam to oxygen carrier ratio.

In addition, less carbon deposition and lower methane conversion can be expected in methane reforming when steam to oxygen carrier ratio increases. The carbon deposition generated in the reaction process came from the decomposition of CH_4. When steam to oxygen carrier ratio rise, H_2O reacted with the deposited carbon to generate CO and H_2, so the carbon deposition was lower under the condition of higher steam to oxygen carrier ratio. It was observed that methane conversion and hydrogen concentration decreased as the methane flow to oxygen carrier ratio increased because in the high methane flow, oxygen carrier does not have enough active sites to react with the excessive methane, which causes a decrease in methane conversion (Hu *et al* 2021c). In comparison to steam methane reforming and methane partial oxidation, the DRM of methane maintains a ratio of H_2/CO equal to 1, which enables better production of oxygenated chemicals and hydrocarbons (Usman *et al* 2015). In DRM of methane, the ratio of H_2/CO increases and gets closer to unity as temperature increases up to 800 °C due to the endothermic nature of the process (Hassani Rad *et al*

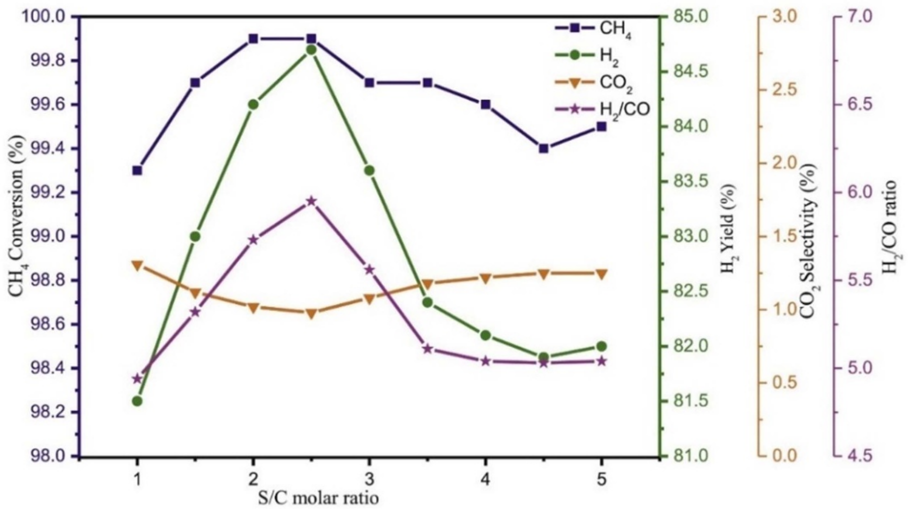

Figure 1. Methane conversion, hydrogen yield, CO_2 selectivity and H_2/CO ratio at 650 °C as a function of Steam/Carbon molar ratio. Reprinted from Nazari *et al* (2021), Copyright (2021), with permission from Elsevier.

2016). The reverse water-gas shift reaction and CO_2/CH_4 ratio plays important roles in the DRM of methane without O_2 addition. Chein and Fung (2019) concluded that by increasing CO_2/CH_4 amount in feedstock, methane conversion increases while H_2 yield decreases.

The steam to carbon ratio is an important factor in defining the methane and product distribution pathways in CLR of methane. The high concentration of steam in the process is not favored as it increases the operating costs and reduces the energy efficiency of the system. Therefore, an appropriate value of steam/carbon ratio should be considered. The changes in methane conversion, product selectivity and syngas ratio was evaluated by Nazari *et al* (2021) as illustrated in figure 1.

The increasing the bed height over fuel reactor is beneficial for the reforming application with natural gas as fuel in a fluidized bed reactor due to an enhancement in methane conversion. This behavior can be explained by the fact that the high bed height means an increase in residence time, which is favorable to the oxidation of surface carbide from the dissociation of methane (Dai *et al* 2012). Further research on impact of temperature in CLR of methane was undertaken by Iglesias *et al* (2017). It was reported that as reaction temperature increases, CO selectivity increases, owing to bulk oxygen mobility being favored in high-temperature conditions. Furthermore, the hydrogen yields, and methane conversion increased with temperature. Compared to $NiO/NiAl_2O_4$, $NiO/MgAl_2O_4$ exhibit better reforming properties, higher methane conversion and higher stability against carbon formation in a fluidized bed reactor at 950 °C (Johansson *et al* 2008).

Operating pressure is another important parameter that should be taken into consideration because of its effect on product distributions in CLR. It was reported that CO_2 and CH_4 conversions decrease when pressure increases from 1 bar to 25 bar. Therefore, it is suggested to operate CO_2 reforming of methane at atmospheric pressure to achieve high syngas yield and conversions (Nikoo and Amin 2011). Furthermore, carbon deposition significantly increases with a rise in pressure. However, Spallina *et al* (2017) tested CLR in packed-bed reactors with integrated CO_2 capture at high pressure around 20 bar and a temperature range from 600 to 900 °C. A CH_4 conversion of 92% during reforming was reported with near-zero CO_2 emissions. They proved that the combination of chemical looping combustion and steam reforming can be accomplished through sequential heat storage and heat removal. Argyris *et al* (2022) successfully demonstrated a CLR packed bed reactor and observed that pressure is a key factor in oxidation in low-velocity operation where higher pressures produced better solid conversion.

The summary of this section is as follows:

- Pure iron oxides cannot meet the requirements of methane reforming in terms of CH_4 conversion and hydrogen selectivity.
- The addition of Ni, Cu and Co to iron-based oxygen carriers exhibits a positive effect on the hydrogen purity in CH_4 reforming processes.
- Among Ni, Fe, Mn, Cu and Co, both Ni and Cu-based oxygen carrier exhibit high reactivity whereas their selectivity toward partial oxidation of CH_4 for syngas production is poor; Fe and Ce based oxygen carrier

possess high selectivity of CO and H_2 toward partial oxidation of CH_4, but their reactivity is low toward CH_4.

- To choose the right reactor configuration, heat transfer rates, reaction kinetics, and the desired extent of reduction of the oxygen carriers should be considered.
- By increasing temperature in fuel reactor, CO selectivity, the hydrogen yields and methane conversion increase.
- The carbon deposition increases with a rise in operating pressure.
- Increasing the bed height over fuel reactor is beneficial for the reforming application in fluidized bed reactors.
- Fluidized bed reactors can improve the methane conversion rate and syngas selectivity compared to the fixed bed reactors.

2.2. CLR of ethanol

Hydrogen can be produced from various types of hydrocarbon and oxygenated-hydrocarbon compounds. Although the main experience of obtaining hydrogen by the CLR process is with gaseous fuels like methane, liquid fuels are becoming more relevant in the last years. Less hazardous, high energy density, relatively high storage safety and transportation, low cost and high availability make ethanol a renewable and carbon-neutral candidate to produce hydrogen (Saupsor *et al* 2020). The hydrogen production from ethanol in the CLR approach over Me_xO_y oxygen carrier consists of three main mechanisms as follows (Saupsor *et al* 2021):

Thermal decomposition of ethanol:

$$C_2H_5OH \rightarrow CO + CH_4 + H_2 \tag{R-7}$$

$$C_2H_5OH \rightarrow C_2H_4 + H_2O \tag{R-8}$$

$$C_2H_5OH \rightarrow CH_3CHO + H_2. \tag{R-9}$$

Ethanol partial oxidation:

$$C_2H_5OH + Me_xO_y \leftrightarrow 2CO + 3H_2 + Me_xO_{y-s}. \tag{R-10}$$

Ethanol steam reforming:

$$C_2H_5OH + 3H_2O \rightarrow 2CO_2 + 6H_2. \tag{R-11}$$

The produced CO can further react with H_2O via a water-gas shift reaction as follows:

$$CO + H_2O \rightarrow CO_2 + H_2. \tag{R-12}$$

For ethanol reforming Ni and Rh-based materials are the most studied oxygen carriers due to their high hydrogen selectivity. For example, ethanol can be fully converted into gaseous products, composed mainly of H_2, CH_4, CO, and CO_2 over CuO–NiO material. Furthermore, the addition of Cu metal into Ni improves the hydrogen selectivity and decreases CO concentration from ethanol. Dou *et al* (2018) obtained hydrogen selectivity of 97% and ethanol conversion in a range of 82%–93% at 873 K over NiO/Al_2O_3. The experimental values of hydrogen production in their investigation were lower than those by equilibrium calculations, which could be due to the oxygen carrier reduction effects to consume the ethanol feeding. Although Ni shows an attractive candidate for CLR of ethanol, some researchers observed carbon deposition on the catalyst surface (Saupsor *et al* 2021).

López Ortiz *et al* (2015) conducted a thermodynamic analysis and concluded that in the ethanol reforming process over NiO oxygen carrier, the maximum hydrogen content occurred in a temperature range of 625 °C–679 °C. Furthermore, CO_2 mols followed the same trend as H_2 content, while CO and CH_4 content reduced. This behavior is consistent with the promotion of the water gas shift and the steam reforming of methane reactions by increasing temperature. One of the advantages of utilizing ethanol over Ni-based materials is the absence of deactivation processes by sulphur that normally happens when fossil fuels are used. Wang *et al* (2017) showed that Ni-based oxygen carriers offer a better catalytic activity than Mn-based materials for the higher hydrogen yield in CLR of ethanol.

The product yield in ethanol reforming not only depending on the type of oxygen carrier but also depending on operating parameters such as temperature, water to ethanol ratio and oxygen to ethanol ratio.

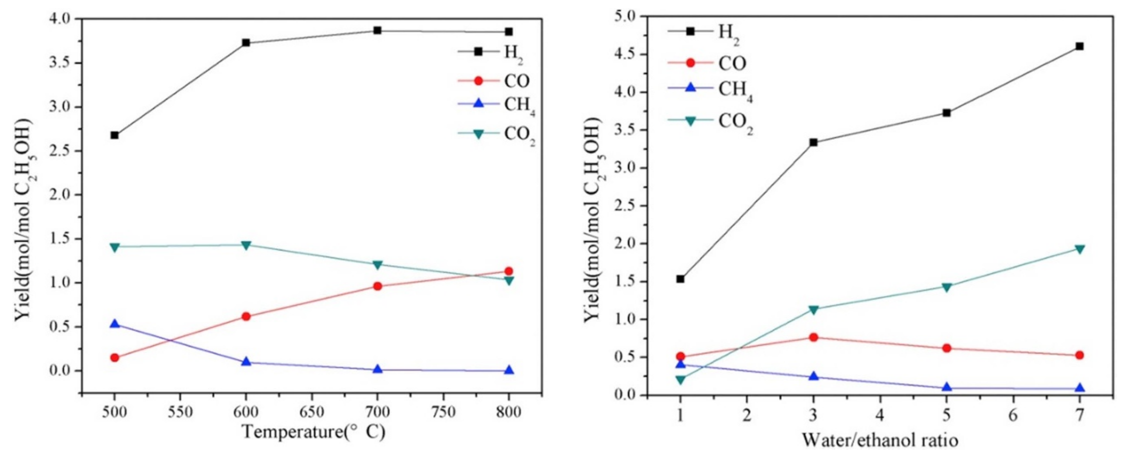

Figure 2. (a), (b) The products yield in chemical looping reforming of ethanol. Reprinted from Wang *et al*, Copyright (2017), with permission from Elsevier.

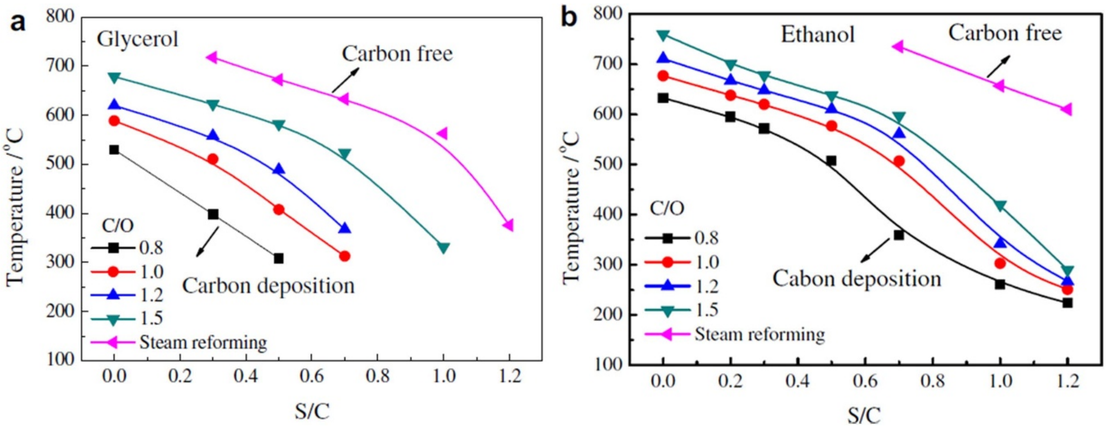

Figure 3. Comparison of chemical looping reforming of glycerol and ethanol. Reprinted from Yang *et al*, Copyright (2011), with permission from Elsevier.

Figure 2(a) indicates that at 500 °C, methane exhibited its highest yield while hydrogen offered its lowest yield, which means ethanol decomposition was one of the main reactions at this temperature. When the temperature increases from 500 °C to 600 °C, the hydrogen yield increased significantly, but the methane yield decreased suddenly indicating ethanol decomposition is not the main reaction anymore. According to figure 2(b), the water/ethanol molar ratio seems to have a strong influence on hydrogen yield at 600 °C. As the water/ethanol ratio increases, H_2 and CO_2 yield increase continuously. The CO and CH_4 yield decrease with a rise in the molar ratio from 3 to 7. It can be concluded that methane reforming and water gas shift (WGS) were promoted. When water/ethanol ratio increases to 7, the methane yield remains constant. García-Labiano *et al* (2015a) claimed that an increase in the oxygen to ethanol ratio reduces hydrogen concentration and increases CO_2 concentration over NiO/Al_2O_3.

The thermodynamic investigations conducted by Yang *et al* (2011) showed that hydrogen selectivity from ethanol reforming is higher than that from glycerol reforming at 650 °C. It was also found that more water has to be consumed in glycerol reforming to achieve the same hydrogen selectivity, which causes a higher energy cost to vaporize water. It may be due to the higher O/C ratio in a glycerol molecule. The more abundance of O in the glycerol system limits the water-gas shift reaction (WGSR) and enhances the oxidation of H_2, which lower the extent to extract hydrogen from water. Therefore, from the view of producing hydrogen ethanol reforming is more efficient than glycerol reforming. Furthermore, the authors concluded that glycerol reforming is more resistant to carbon deposition as the coke is formed at lower temperatures in ethanol reforming compared to glycerol reforming as given in figure 3. This can be explained by the more oxygen atoms in glycerol molecule than in ethanol, which facilitates the formation of gaseous CO or CO_2.

The key messages of this section can be summarized as follows:

- Ni and Rh-based materials are the most common oxygen carriers in ethanol reforming due to their high hydrogen selectivity.
- The addition of Cu metal into Ni improves the hydrogen selectivity and decrease CO concentration.
- In the ethanol reforming over NiO, the maximum hydrogen content occurs in a temperature of 625 °C–679 °C and at water/ethanol ratios of 6 and 3.
- The hydrogen selectivity from ethanol reforming is higher than that from glycerol reforming at 650 °C.
- An increase in the oxygen-to-ethanol molar ratio reduces hydrogen concentration and increases CO_2 concentration.
- Ni-based oxygen carriers offer a better catalytic activity than Mn-based materials for the higher hydrogen yield in ethanol reforming system.
- The water to ethanol molar ratio showed a strong influence on hydrogen yield.

2.3. CLR of glycerol

Biodiesel production around the world had experienced a huge increase in the last years. Glycerol, as the main by-product, is produced by the conversion of animal-based or vegetable oils into biodiesel through the catalytic trans-esterification process. Although the purification process of glycerol is expensive and complicated, crude glycerol must be purified before it can be used due to its impurities (Suero *et al* 2015). To address this issue, the hydrogen production technology of glycerol steam reforming due to its good industrial application prospects has increasingly attracted increased attention in the past decades. It is noteworthy to mention that methane is a non-renewable resource, hence glycerol might be an attractive option due to its renewability. The catalyst-to-feed ratio, steam-to-carbon ratio and temperature are the most important factors in the glycerol steam reforming process while major concerns are high energy consumption, byproduct formation and catalyst deactivation (Iliuta and Iliuta 2013). Steam reforming of glycerol is the most well-known and preferable technique for H_2 production because it can theoretically make 7 mol of H_2 with the consumption of 1 mol glycerol (Patcharavorachot *et al* 2019) as follows:

$$C_3H_8O + 3H_2O \rightarrow 3CO_2 + 7H_2. \tag{R-13}$$

The following side reactions also take place during glycerol steam reforming which might affect the yield and selectivity of the target product (Qingli *et al* 2021). The used oxygen carriers for glycerol reforming should have the ability to break the C–C, C–H and H–O bonds and promote the water-gas shift reaction to form hydrogen and CO_2 as well as it should maintain the ability of C=O bonds, which improves the selectivity of hydrogen.

Glycerol pyrolysis:

$$C_3H_8O \rightarrow CH_4 + H_2O + H_2 + 2CO. \tag{R-14}$$

Water-gas shift reaction:

$$CO + H_2O \rightarrow CO_2 + H_2. \tag{R-15}$$

Methanation reactions

$$CO + 3H_2 \rightarrow CH_4 + H_2O \tag{R-16}$$

$$CO_2 + 4H_2 \rightarrow CH_2 + 2H_2O \tag{R-17}$$

methane decomposition:

$$CH_4 \rightarrow C + 2H_2. \tag{R-18}$$

CO disproportionation reaction:

$$2CO \rightarrow CO_2 + C. \tag{R-19}$$

Ni-based oxygen carriers with a low cost and strong ability to break O–H, C–H and C–C bonds have been evaluated for utilization in glycerol reforming processes. A comparative study by Adhikari *et al* (2007) on glycerol conversion and product composition over various oxygen carriers in CLR of glycerol showed that the glycerol **c**onversion can be ranked in the order Ni > Ir > Pd > Rh > Pt > Ru, while hydrogen selectivity was

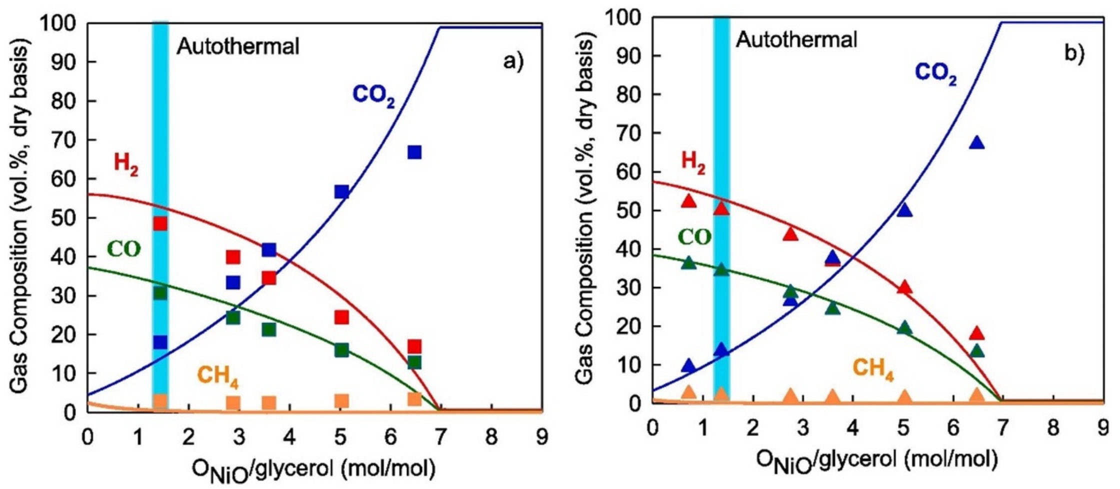

Figure 4. Effect of O_{NiO}/glycerol ratio in the composition of the fuel reactor gas stream at (a) 750 °C; (b) 800 °C. Reprinted from Adánez-Rubio *et al*, Copyright (2021), with permission from Elsevier.

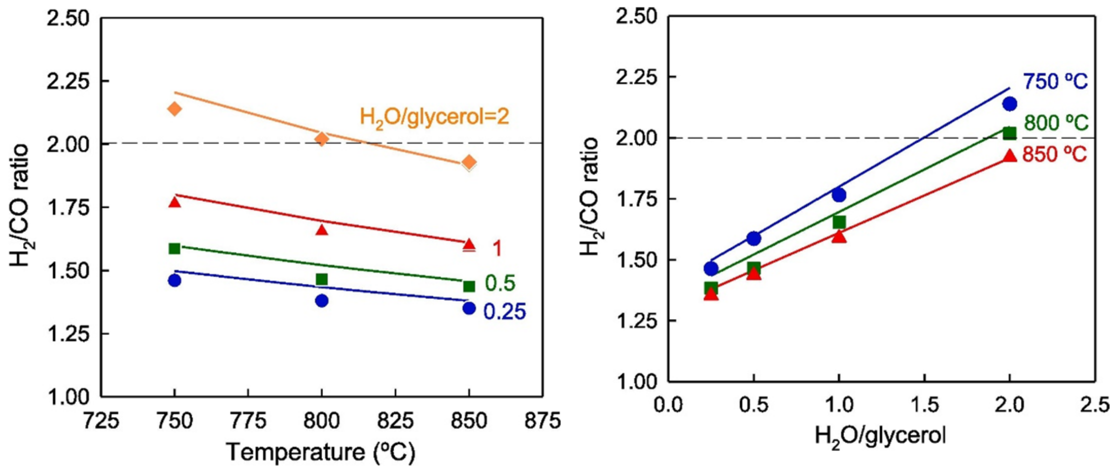

Figure 5. H_2/CO ratio as a function of the fuel reactor temperature and H_2O/glycerol in glycerol reforming. Reprinted from Adánez-Rubio *et al*, Copyright (2021), with permission from Elsevier.

found to be in the order Ni > Ir > Ru > Pt > Rh > Pd. Catalytic conversion of glycerin to H_2, CO_2, and CO involves the preferential cleavage of C–C bonds as opposed to C–O bonds. It is generally accepted that nickel promotes C–C rupture.

The effect of operating variables such as O_{NiO}/glycerol and H_2O/glycerol on the synthesis composition needs to be examined since in CLR process, water addition is utilized to improve hydrogen production as well as to minimize carbon deposition. Figure 4 shows that higher values of H_2 and CO can be obtained at a lower O_{NiO}/glycerol ratio due to the higher contribution of the partial oxidation with respect to the glycerol combustion because of the lower lattice oxygen availability. As given in figure 5, H_2/CO ratio is a strong function of water amount in feedstock. At all temperatures, H_2/CO ratio and CO_2 concentration increase with a rise in H_2O/glycerol ratio from 0.25 to 2 due to the enhancement of the direct glycerol reforming and the water-gas shift reaction. It is evident that the H_2/CO ratio decreases from 2.15 to 1.35 when fuel reactor temperature increases from 750 °C to 850 °C due to the increase in the CO formation while the H_2 remained almost constant with the temperature.

Delparish *et al* (2019) showed full conversion of glycerol can be determined at steam to carbon ratio equal to 5, C/O range of 0.75–1.25, and at temperatures from 550 to 700 °C. Their funding indicated that yields of H_2 and CO_2 increase with the increasing amount of steam in the feed while CO yield decreases. It can be explained by the fact that the WGS reaction is favored at higher amounts of inlet steam to transform CO into H_2 and CO_2.

One of the main parameters in the liquid reforming by CLR technique is oxygen-to-fuel molar ratio as the amount of lattice oxygen transferred by the oxygen carrier in the fuel reactor controls the reforming process and product composition. To achieve lower H_2/CO ratio suitable in downstream, researchers added CO_2 to feedstock in steam CLR of glycerol (Tavanarad *et al* 2021). Feeding glycerol with CO_2 to fuel reactor decreases H_2/CO ratio which can be attributed to the positive effect of the excess CO_2 on the reverse water-gas shift reaction. The glycerol conversion shows higher values at a higher CO_2/glycerol molar ratio.

From an economic point of view, it is not desirable to heat and pumps more water through the system than is necessary. An increase at concentration of glycerol in feed has a positive effect on H_2 yield while decreases CH_4 yield, Byrd *et al* (2008). This can be explained by the fact that at low steam/carbon ratios (high glycerol concentration) CO is more likely to produce methane by consuming hydrogen.

Gas hourly space velocity has a significant effect on glycerol conversion and product composition in glycerol reforming. It was observed that glycerol conversion increases when gas hourly space velocity decreases. The residence time of reactants decreases and the pressure drop of the reactor increases at higher gas hourly space velocity which leads to higher coke formation over the catalysts surface and less glycerol conversion. Based on the results above, the yield of H_2 production in CLR of glycerol depends on oxygen carrier follows the order CuO (81.00%) $<$ NiO (81.07%) $<$ CoO (81.14%) $<$ Co_3O_4 (81.80%) $<$ Fe_2O_3 (83.66%) $<$ Mn_2O_3 (87.33%) $<$ Mn_3O_4 (87.54%) indicating Mn-based materials have great potential in CLR of glycerol applications.

The important conclusions of this section are as follows:

- The most important parameters in the glycerol steam reforming process are temperature, steam-to-carbon ratio, and catalyst-to-feed ratio.
- Major concerns in glycerol reforming are by-product formation, catalyst deactivation, and high energy consumption.
- The glycerol conversion over various oxygen carriers can be ranked in the following: Ni $>$ Ir $>$ Pd $>$ Rh $>$ Pt $>$ Ru.
- The gas hourly space velocity has a significant effect on glycerol conversion and product composition in glycerol reforming.
- The yield of H_2 production in glycerol reforming over various oxygen carriers is in accordance with the order of CuO $<$ NiO $<$ CoO $<$ Co_3O_4 $<$ Fe_2O_3 $<$ Mn_2O_3 $<$ Mn_3O_4.
- H_2/CO ratio in glycerol reforming is a strong function of water amount in feedstock.

3. Recent advances in oxygen carriers for CLR

The solid oxygen carrier materials that are used in chemical looping technologies to transfer oxygen from the air to the fuel have a key role in the success of the process for the production of hydrogen (Hu *et al* 2021b). In this regard, extensive research has been made toward the development of optimum oxygen carrier materials with improved properties which will be discussed in this section. The oxygen carriers can be divided into two main categories including synthetic materials and natural minerals. Although natural minerals are cheap, their reactivity is usually lower than synthetic oxygen carriers (Adanez *et al* 2012). Metal oxides of Fe, Ni, Co and Mn with inert support such as TiO_2, Al_2O_3 and SiO_2 are the most studied synthetic oxygen carriers in the literature which possess their individual advantages and weaknesses. As chemical looping processes are often operate at high temperatures in industrial application, it is critical to select a suitable oxygen carrier based on its thermal stability to avoid material sintering. The melting temperature of several different transition-state metals and their corresponding oxides have been listed in table 3. In addition, the maximum oxygen transport capacity of oxygen carriers was also given in this table. Oxygen carriers with a low circulation rate are suitable from design simplicity and less circulation power point of view. However, it should be high enough to transport sufficient oxygen for complete fuel oxidation as well as to transport the desired heat in case of an endothermic reaction in the fuel reactor (Abuelgasim *et al* 2021).

To ensure the oxygen carriers have desirable qualities, an understanding of the reaction mechanism and morphological changes during the reaction are needed. The various competing factors such as resistance to toxicity, easy scalability, complete fuel conversion to CO and H_2, environmental aspects, low cost, availability, high attrition resistance, high conversion rate, and stability under repeated oxidation/reduction, high oxygen-carrying capacity and good heat-carrying capacity should take into account before selection of an appropriate oxygen carrier (Sun *et al* 2020). However, it is not easy to find a metal oxide that could meet all the above factors. In this regard, supporting materials such as $MgAl_2O_4$, ZrO_2, SiO_2, TiO_2 and Al_2O_3 can be added to metal oxides to improve attrition resistance and mechanical strength. Furthermore, depending on which preparation method is used for oxygen carriers, their properties can change. There are several methods to prepare oxygen carriers including spray pyrolysis, sol-gel, spray drying, pelletizing by extrusion, precipitation, mechanical mixing, impregnation, hydrothermal synthesis, dissolution, freeze granulation, deposition precipitation, co-precipitation and citric acid method (Rydén *et al* 2011, Li *et al* 2020, Long *et al*

Table 3. Melting temperature and maximum oxygen transport capacity of most common oxygen carriers. Adapted from Jerndal *et al* 2006, Adánez *et al* 2018, Adanez *et al* 2012, Copyright (2006, 2012), with permission from Elsevier.

Oxidation/reduction form	Melting temperature (°C)	Maximum oxygen transport capacity
NiO/Ni	1955/1455	0.214
CuO/Cu	1446/1085	0.201
CuO/Cu_2O	1446/1235	0.101
FeO/Fe	1377/1538	0.222
Fe_2O_3/Fe_3O_4	1565/1597	0.034
Fe_2O_3/Fe	1565/1538	0.100
Mn_3O_4/MnO	1562/1842	0.070
Mn_2O_3/Mn_3O_4	1347/1562	0.034
CoO/Co	1830/1495	0.214
Co_3O_4/CoO	1830/1830	0.067
Ce_2O_3/CeO_2	2230/2400	0.048
$BaSO_4/BaS$	1580/2230	0.274
$SrSO_4/SrS$	1607/2227	0.348

2020). Many materials have been investigated in the literature for the chemical looping operation and are presented in the following sections. A summary of different kinds of oxygen carries utilized in chemical looping processes was also listed in table 4.

3.1. Ni-based oxygen carriers

Using nickel-based oxygen carriers for chemical looping concepts has attracted considerable attention from many researchers due to their low cost, high catalytic activity, outstanding oxygen transfer capacity (0.21 g O_2/g NiO) and great thermal stability (Roslan *et al* 2020). The excellent catalytic activity of Ni has been associated with its remarkable ability for breaking the C–C bonds. Ni-based oxygen carriers were the first materials employed for demonstrating the viability of chemical looping as a carbon capture technology. The presence of nickel helps to promote the water-gas shift reaction, leading to an increase in hydrogen production. Nevertheless, they suffer from several limitations such as toxicity and coke formation on the catalyst surface, leading to blockage of nickel active sites and deactivation. A comparison between the reactivity of NiO, Mn_2O_3, Fe_2O_3 and CuO metal oxides showed that the reactivity of NiO with methane is the highest while Fe_2O_3 offer the lowest reactivity followed by CuO (Zafar *et al* 2005). In addition, NiO/SiO_2 exhibit the highest selectivity toward hydrogen production compared to others. The reason for the low reaction rate of CuO/SiO_2 is the decomposition of CuO to Cu_2O during the inert period following the oxidation, which means that less oxygen is available for the oxidation of the fuel. It was reported that the implementation of CO_2 sorption in CLR can increase the purity of hydrogen by more than 90% and decrease the operating temperature, resulting in an improvement in the stability of the Ni. The performance of Ni-based material depends significantly on metal supports that are used in catalyst preparation. It was shown that a high activity can be determined using $MgAl_2O_4$ as metal support. Metal supports of SiO_2 and Al_2O_3 are better candidates in terms of high temperature stability (Nieva *et al* 2014).

In CLR processes, material deactivation caused by carbon deposition is one of the main issues. The several techniques such as using dry impregnation method to prepare catalyst, the addition of a small amount of alkali metals (K, Mg, Ca), type of support and the addition of a small amount of steam to the reactor were proposed in the literature to reduce carbon deposition on the material surface (Elias *et al* 2013). For example, it was found that ceria-supported catalyst exhibits the lower carbon deposition compared to MgO, TiO_2. Ceria establishes a better interaction with the Ni active phase, which causes a higher metal dispersion and inherently available surface area.

Tavanarad *et al* (2021) employed 15 wt% Ni supported on Al_2O_3 with 3 wt% promoters such as MgO, CaO, SrO, and BaO in the glycerol reforming. Figure 6 shows glycerol conversion of Ni catalysts at a temperature range from 600 to 750 °C with and without promoters. As can be seen from the figure, all promoters increased the glycerol conversion and among them, SrO exhibited the highest glycerol conversion. The authors explained that this improvement could be related to the adsorption of CO_2 on the catalysts and the smaller crystallite sizes of the promoted catalysts. Furthermore, higher glycerol conversion on the promoted catalysts can be attributed to the enhanced basic properties of the catalysts. The addition of alkaline earth metal oxide promoters improves the adsorption of CO_2 on the catalysts and inhibits the Boudouard reaction, and suppresses the coke formation. The temperature showed a significant effect on glycerol conversion as it increases when temperature increases from 600 to 750 °C due to endothermic nature of the reaction.

Table 4. Summary of the oxygen carriers tested in different chemical looping reforming units.

Metal carrier	Support material	Synthesis method	References
Fe, Mn, Co, Cu	Al_2O_3	Co-precipitation	Forutan *et al* (2015)
Fe, Ni, Mn	Al_2O_4	Impregnation	Svoboda *et al* (2008)
Fe	Al_2O_4	Commercial	Lu *et al* (2021)
Cu	Al_2O_4	Commercial	Guo *et al* (2015)
Cu	Al_2O_3	Incipient wetness impregnation	Keller *et al* (2016)
Cu	Al_2O_3	Co-precipitation	Alirezaei *et al* (2016)
Ni	γ Al_2O_3	Impregnation	Rydén *et al* (2008)
Ni	a Al_2O_3	Incipient wetness impregnation	Garcia-Labiano *et al* (2014)
Ni	Al_2O_3	Commercial	Yahom *et al* (2014)
Fe–Cu	Al_2O_3	Commercial	Siriwardane *et al* (2015)
Fe, Ni, Co	CeO_2	Impregnation, Co-precipitation	Guerrero-Caballero *et al* (2019)
Fe–Ni	Al_2O_3	Co-precipitation	Wei *et al* (2019)
Fe	Al_2O_3	Sol-gel synthesis	Solunke and Veser (2010)
CeO_2	γ Al_2O_3	Incipient wetness impregnation	Wei *et al* (2007)
Ni–Cu	Al_2O_3	Hydrothermal syntheses	Huang *et al* (2019)
Co	CeO_2	Wet-impregnation	Ayodele *et al* (2016)
Cu	γ Al_2O_3	Incipient wet impregnation	Forero *et al* (2011)
Ni–CeO_2	Al_2O_3	Co-precipitation	Shamskar *et al* (2017)
Ni–CeO_2	Al_2O_3	Incipient wetness impregnation	Chein and Fung (2019)
Ni–Ce	MgO	Impregnation	Khajenoori *et al* (2015)
Ni	SiO_2, Al_2O_3	Incipient wetness impregnation	Nieva *et al* (2014)
Ni, Co, Cu	SiO_2	Incipient wetness impregnation	Papageridis et al (n.d.)
Ni, Co, Cu	γ Al_2O_3	Incipient wetness impregnation	Papageridis *et al* (2016)
Co	Al_2O_3	Commercial	Jerndal *et al* (2006)
CuO	TiO_2	Self-assembly combustion synthesis	Tian *et al* (2020)
CuO	ZrO_2	Incipient wetness impregnation	Adánez-Rubio *et al* (2020)
Fe_2O_3	Al_2O_3	Sol-gel synthesis	Kang *et al* (2019)
CeO_2	Fe_2O_3	Chemical precipitation	Zhu *et al* (2014)
Fe_2O_3/CeO_2	ZrO_2	Co-precipitation	Yamaguchi *et al* (2011)
CeO_2	ZrO_2	Precipitation	Jang *et al* (2014)
NiO, CuO, Fe_2O_3	SiO_2	Dry impregnation	Zafar *et al* (2005)
NiO	ZrO_2, TiO_2, SiO_2	Dry impregnation	Antzara *et al* (2016)
Cu–Fe	Al_2O_4	Co-precipitation	Imtiaz *et al* (2015)
Ni–Fe	Al_2O_4	Co-precipitation	Huang *et al* (2018)
Cu–Ni	Al_2O_3	Impregnation	Khzouz *et al* (2013)
Cu–Fe	Al_2O_3	Impregnation, Co-precipitation	Chiron and Patience (2012)
Cu	Al_2O_3	Wet-impregnation	Zheng *et al* (2014)
CeO_2	N.A.	Precipitation	Zhu *et al* (2011)
Ni	CeO_2, La_2O_3	Co-precipitation, Impregnation	Pantaleo *et al* (2015)
$Ce_xFe_{10\text{-}x}O$	N.A.	Citric acid sol-gel method	Yan *et al* (2018)
Fe–Ni	CeO_2	Impregnation	Luo *et al* (2022)
CeO_2	BF_3	Chemical co-precipitation	Cheng *et al* (2021)
NiO	$CeZrO_4$	Impregnation	Zhang *et al* (2021b)
Ni, Co, Cu, Fe	$MgAl_2O_4$	Co-precipitation	Hu *et al* (2021a)
Ni–Fe	Calcite	Wet-impregnation	Hu *et al* (2021c)
Fe–CeO_2	N.A.	Sol-gel Pechini method	García-García and Metcalfe (2021)
Ni	γ Al_2O_3	Impregnation	Tavanarad *et al* (2021)
Ni–Mg	ATP	Impregnation	Qingli *et al* (2021)
NiO	Al_2O_3	Co-precipitation	Dou *et al* (2017)
Fe_2O_3	Al_2O_3	Mechanical mixing method	Ma *et al* (2020)
Ni	CeO_2	Co-precipitation	Han *et al* (2022)
Co	Mg_3Al	Calcination	Li *et al* (2018a)
CeO_2	$LaFeO_3$	Gas-bubble-assisted method	Zheng *et al* (2017)
Mn_3O_4	$MgZrO_3$	N.A.	Lind *et al* (2012)
Fe_3O_4	Al_2O_3	Commercial	Abdalazeez *et al* (2021)
Mn	ZrO_2	Co-precipitation	Alirezaei *et al* (2018)
CeO_2–CuO	ZrO_2	Sol-gel method	Wang *et al* (2019)
Co–Fe_2O_3	N.A.	Sol-gel method	Guo *et al* (2020)
Ce–Ni	PSNT	Alkalinity-tuned hydrothermal	Jiang *et al* (2018a)
Ni–Fe_2O_3	Al_2O_3	Impregnation	Kang *et al* (2018)

(Continued.)

Table 4. (Continued.)

Ba–Co	CeO_2	Sol-gel method	Ding *et al* (2019)
Ni–Fe	N.A.	Co-precipitation	Huang *et al* (2016)
CuO–NiO	Al_2O_3	Hydrothermal method	Wang *et al* (2018)
CuO, Fe_2O_3	Al_2O_3	Sol-gel method	Zhao *et al* (2015)
Fe_2O_3	$MgAl_2O_4$	Co-precipitation	Hafizi *et al* (2016)
CeO_2	ZrO_2	Co-precipitation	Zheng *et al* (2016)
Fe_2O_3	Al_2O_3	Co-precipitation	Zhu *et al* (2019)
Ni	Mn_2O_4	Sol-gel method	Wang *et al* (2017)
Cu–Fe	Al_2O_3	N.A.	Nadgouda *et al* (2019)
Ni–CeO_2	Al_2O_3	Wet-impregnation	Isarapakdeetham *et al* (2020)
Ce–Fe	MgAl	Co-precipitation	Yuan *et al* (2020)
Ni–Cu/Fe_2O_4	N.A.	Sol-gel method	Chen *et al* (2019)

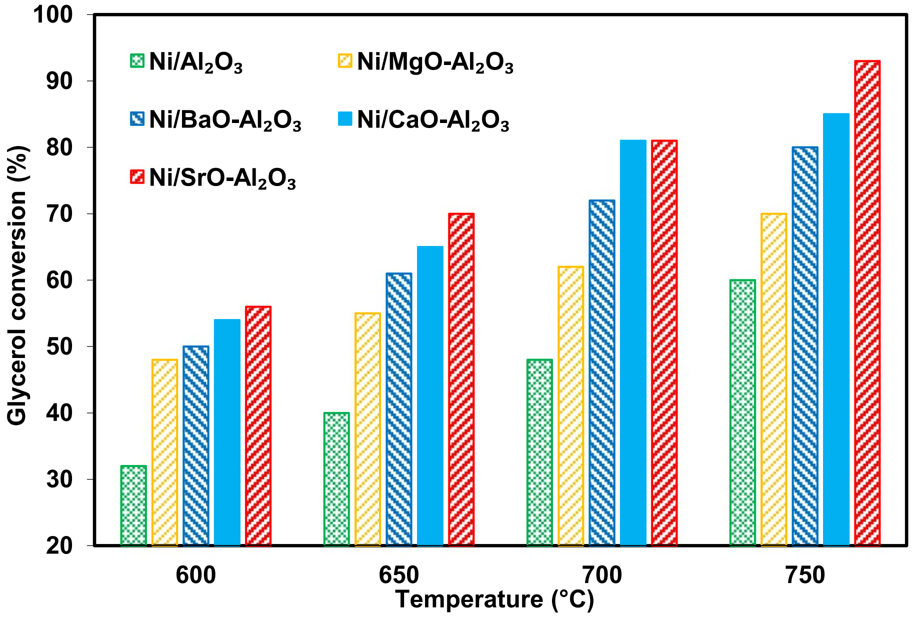

Figure 6. The glycerol conversion of the 15 wt% Ni catalyst as a function of temperature and different promoters. Adapted from Tavanarad *et al*, Copyright (2021), with permission from Elsevier.

3.2. Fe-based oxygen carriers

The environment friendliness, low price and good redox properties make iron-based oxygen carriers an attractive candidate for the chemical looping process (Lu *et al* 2021). Furthermore, iron-based materials exhibit high melting points, and high mechanical strength and have no tendency for carbon formation or sulphide/sulphate formation. Although they offer acceptable reactivity for hydrogen and carbon monoxide, they have weak reactivity for methane (Yu *et al* 2019). Similar to other oxygen carriers, iron-based materials also have a few drawbacks including low oxygen transport capacity and the complexity of heat management due to their endothermic nature (Li *et al* 2019b). Moreover, ash compositions could react with an iron oxygen carrier which results in sintering and agglomeration (Bao *et al* 2014). Generally, iron-based oxygen carriers are composed of primary iron oxide for lattice oxygen storage and ceramic support for improved redox stability and activity.

Evolution of iron oxide during reforming and reduction was given in figure 7. During the reduction step, Fe_2O_3 is reduced by gaseous fuel in order to desorb oxygen for CO_2 formation and obtain adequate active sites for catalytic DRM of methane. In the DRM step, CH_4 and CO_2 gases are fed and the catalyst reaction of DRM and POM occur on the active site for syngas production along with oxygen migration. Iron-based oxygen carriers exhibit the maximum capacity for oxygen adsorption and the highest resistance against sintering compared to Co, Cu and Mn-based oxygen carriers. The optimum temperature of cobalt, magnesium, copper and iron metal oxides supported on alumina are 1298 K, 1073 K, 1303 K and 1173 K, respectively (Forutan *et al* 2015). Lu *et al* (2021) studied the behavior of magnetite with Fe_3O_4 in reforming of methane and observed that the temperature rise is beneficial to the reduction of iron oxide in the fuel reactor. Guerrero-Caballero *et al* (2019) performed a comparative study on several ceria-based oxygen

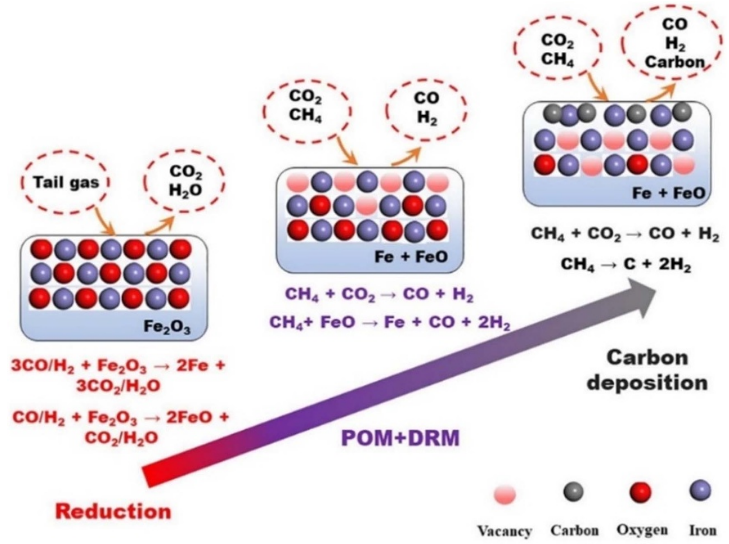

Figure 7. The evolution of iron oxide during the reduction and dry reforming stages. Reprinted from Zhu *et al*, Copyright (2019), with permission from Elsevier.

carriers such as Ni, Co and Fe in reforming of methane. It was found that at a temperature around 873 K, Co/CeO_2 shows promising results while Fe-based oxygen carrier exhibits better performance at higher temperatures. Therefore, iron-based material might be a better candidate than nickel in terms of toxicity and environmental reasons. Solunke and Veser (2010) claimed that iron metal oxide is the best option from a melting point, cost, toxicity and reduction cycle point of view. The deactivation of iron oxide over multiple redox cycles is one of their limitations which leads to a decrease in CO selectivity. Moreover, the formation of CO_2 during the reduction of Fe_2O_3 to Fe_3O_4 leads to a decrease in CO selectivity and the productivity of value-added fuels generated. The combination Fe and Ce has been suggested by several researchers due to positive effect of the addition of Ce (García-García and Metcalfe 2021). It was reported that Fe–Ce mixed oxides produce pure hydrogen and high-quality syngas due to a strong interaction between CeO_2 and Fe_2O_3 species which greatly enhances the mobility of oxygen in the Ce–Fe and improves the oxygen vacancies through the formation of $CeFeO_3$ phases. Furthermore, the addition of CeO_2 to Fe oxide leads to higher hydrogen and CO yields due to synergetic interaction between both cerium and iron oxides and the formation of a peruskite type oxide. Therefore, by controlling the amount of metal oxide in the mixture, product selectivity can be adjusted.

3.3. Cu-based oxygen carriers

Cu-based oxygen carriers with attractive properties have been widely studied in the literature. Great oxygen transport capacity, low toxicity, high reactivity in both reduction and oxidation cycles as well as moderate cost make Cu-based materials one of the most known oxygen carriers in chemical looping processes (Abad *et al* 2007). One of the interesting advantages of this type of material is that reduction and oxidation reactions are exothermic which results in no heat supply energy requirement in the reduction reactor. Furthermore, sulphurous impurities in the fuel do not significantly affect the properties of Cu oxygen carriers (Forero *et al* 2010). However, the main issue with Cu-based material is their relatively low melting point which results in agglomeration problems.

Agglomeration of oxygen carriers usually occurs when particles of oxygen carriers adhere to one another and form clusters which results in a reduction in material stability and reaction rate. To make Cu-based material a more attractive oxygen carrier, it is essential to improve its performance at high temperatures. This can be achieved using different preparation methods and addition inert supports.

For example, the efficiency of Cu oxygen carriers can be improved by the addition of 20% zirconium oxide. The 15Cu/20Zr–Al showed the highest catalytic activity with 99.2% methane conversion at 923 K. Moreover, it was found that the Zr content in the support structure could affect the coke deposition on the Cu-based oxygen carrier surface. The volumetric percentage of CO and CO_2 in the reactor effluent could be related to the content of coke deposited on the oxygen carrier surface. The presence of CO and CO_2 in the oxidation section is related to the burning of coke in the oxidation period. By increasing the Zr loading weight percentage, the emission of CO and CO_2 is decreased. The emitted CO_2 is reduced from about 47% to 3% by increasing the zirconium loading from 0% to 20% in the oxygen carrier support structure. Further

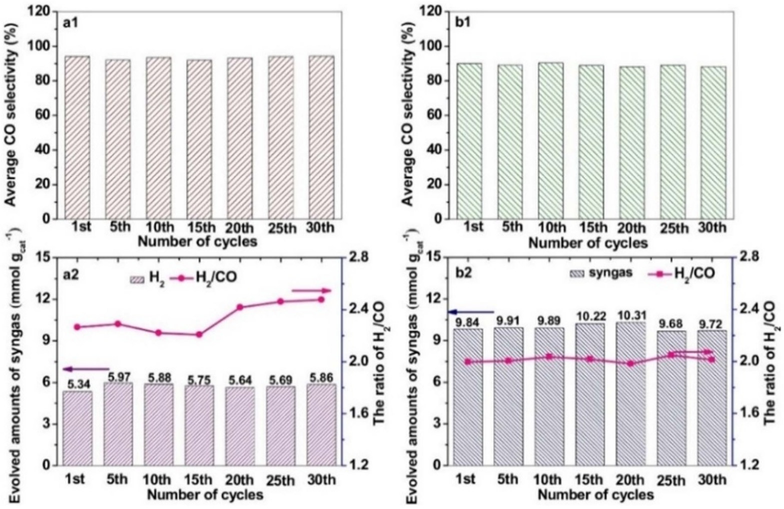

Figure 8. CO selectivity and syngas yield during the chemical looping reforming of methane over $LaFeO_3$ (a1), (a2) and 10%$CeO_2/LaFeO_3$ (b1), (b2). Reprinted from Zheng *et al*, Copyright (2017), with permission from Elsevier.

increase in the Zr loading tends to increase the CO_2 percentage (Alirezaei *et al* 2016). The dry impregnation of porous supports may be a better production technique compared to spray drying for CLR bed materials due to good dispersion of the active Cu phase.

Although using CuO at high temperatures was always rejected in the literature, it was observed that an increase in the oxidation temperature up to 1173 K is feasible with CuO without any deactivation or agglomeration of the particles (Forero *et al* 2011). The addition of Fe to Cu was proposed to improve material mechanical stability while maintaining a high reactivity in oxidation as well as reduction. Furthermore, combining CuO with Fe_2O_3 can limit the temperature drop in the fuel reactor as CuO releases heat and Fe_2O_3 reacts endothermic (Chiron and Patience 2012).

3.4. Ce-based oxygen carriers

In the DRM of methane process, good resistance to coke is critical for catalysts and favorable from an economic point of view. Ceria-based catalysts exhibit high resistance to coke formation and have unique redox properties. Thanks to its great redox capacity, ceria is the most interesting oxide in the chemical looping POM (Li *et al* 2019a). Furthermore, CeO_2 is very attractive in chemical looping due to the formation of Ce^{3+} sites and CeO_2 oxygen vacancies, which improves the performance of various reactions. Jang *et al* (2014) used ZrO_2 as support for CeO_2 and indicated an improvement in temperature stability, redox performance and oxygen storage capacity. The production of syngas and hydrogen on CeO_2–ZrO_2 was found to be about twice that of pure CeO_2 and not race of carbon deposition was observed.

Zheng *et al* (2017) used $LaFeO_3$-supported CeO_2 as an oxygen carrier and their results revealed that the presence of CeO_2 improves the resistance toward carbon deposition formation, and this allows the oxygen carrier own high available oxygen storage capacity. As shown in figure 8, pure $LaFeO_3$ exhibits H_2/CO ratio of around 2.4 in the produced syngas while $CeO_2/LaFeO_3$ showed H_2/CO ratio near 2 meaning the formation of carbon deposition in $CeO_2/LaFeO_3$ is avoided. Since the stoichiometric reaction of a CH_4 molecule with oxygen should yield a H_2/CO ratio of 2.0, ratios higher than 2 indicates the decomposition of CH_4 which would result in the formation of carbon deposition. Furthermore, CO selectivity for $LaFeO_3$ and 10%$CeO_2/LaFeO_3$ materials was also reported to be about 90% during the 30 redox cycles at 800 °C. Syngas yield for 10%$CeO_2/LaFeO_3$ (9.72 mmol g^{-1}) was found to be much higher than that over the pure $LaFeO_3$ (5.86 mmol g^{-1}) and it is very stable during the redox testing.

3.5. Mn-based oxygen carries

From a reactivity, cost, temperature stability and environment point of view, manganese oxide seems a potential oxygen carrier (Nandy *et al* 2016). Although manganese presents a low oxygen transport capacity, their oxygen transport capacity is still greater than Fe-based materials. Mn, MnO, MnO_2, Mn_2O_3 and Mn_3O_4 are oxidation states of Mn-based oxygen carriers. Among them, Mn_3O_4 is the only Mn species that shows its presence at temperatures higher than 1073 K. Mn_2O_3 is thermodynamically stable in air at temperatures lower than 1173 K and MnO_2 is the highest oxidation state of Mn which can be used as an oxygen carrier, tends to start decomposition in the air at about 773 K (Johansson *et al* 2006). To date, few studies about

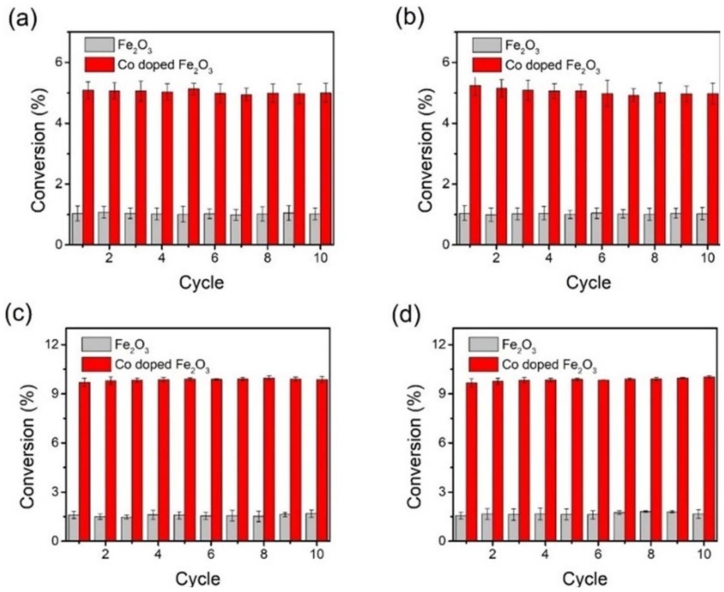

Figure 9. The effect of the addition of 2% cobalt to iron-based oxygen carrier in chemical looping reforming at 600 °C for, (a) reduction and (b) oxidation, at 700 °C for (c) reduction and (d) oxidation. Reprinted from Guo et al, Copyright (2020), with permission from Elsevier.

using Mn-based materials can be found in the literature. Alirezaei *et al* (2018) prepared a manganese-based oxygen carrier on ZrO_2 support and applied it to production of syngas. Based on their results, 20%Mn/20%Zr–Al reveals great redox activity, good structural properties, and stability with a methane conversion of about 97.0% at 650 °C and 99.9% at 750 °C. The significantly higher activity of 20Mn/20Zr–Al oxygen carrier could be due to high surface area, better dispersion of manganese oxide, reduction in the particle size of manganese oxide and the superior interactions between Mn and Zr–Al. The reduction in H_2/CO molar ratio with temperature for Zr promoted samples could be related to reverse water gas shift reaction, which increases the concentration of carbon monoxide with the consumption of hydrogen. A maximum of methane and carbon dioxide conversion is obviously obtained by increasing the Mn loading percentage up to 20%. Correspondingly, the catalytic activity is decreased by further increase of active phase loading. Further increase in Mn loading percentage might intensify the agglomeration and pore blockage, which has negative effect on its activity.

3.6. Co-based oxygen carries

In general, Co has a few oxidation states such as Co_3O_4, CoO and Co during the redox operation. At a temperature higher than 1173 K, Co_3O_4 is unstable and easily convert into CoO. Among the possible metal oxides for chemical looping technology, cobalt shows the highest oxygen transport capability (Hossain and de Lasa 2008). Therefore, Co-based material might be better choice from an oxygen transport capacity point of view. High melting temperature and fast reactivity are other advantages of this type of material. However, their drawbacks include negative health effects and high cost which limits their application in large-scale operations (Abuelgasim *et al* 2021). The existing literature pertaining to the production of syngas from chemical looping technologies over Co-based material remains scarce.

DRM of methane was studied using CeO_2-supported Co catalyst in a fixed bed reactor by Ayodele *et al* (2016). Their results revealed that 20 wt% Co/80 wt% CeO_2 has the potential to be used for production of CO-rich hydrogen which is favorable for the production of other value-added chemicals. Li *et al* (2018a) examined Co catalyst with MgAl support for low-temperature methane reforming and observed that the Co catalyst shows high coke resistance and stable activity due to its lower activity for CH_4 dissociation/decomposition and its stronger metal-support interaction. Guo *et al* (2020) studied the role of Co in chemical looping using iron oxide as an oxygen carrier at a temperature ranging from 600 to 800 °C. As can be seen in figure 9, the methane conversion increased by around 300% for Co-doped iron oxide compared to pure iron oxide oxygen carriers. Furthermore, Co-doping-induced oxygen vacancy significantly reduces energy barriers of CH_4 reforming on the surface of iron oxide oxygen carriers, leading to reactivity enhancement.

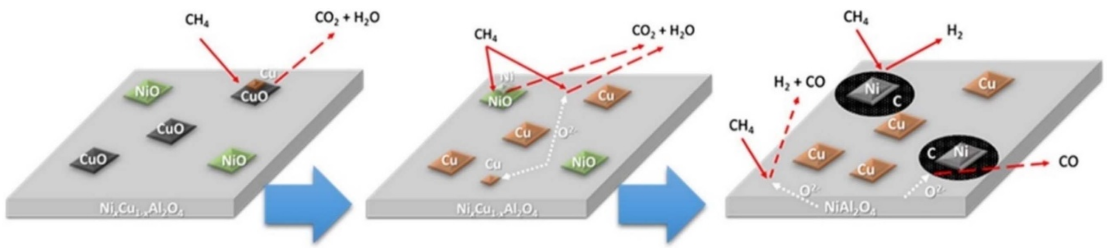

Figure 10. A schematic diagram of the reaction sequence. Reprinted from Huang *et al*, Copyright (2019), with permission from Elsevier.

3.7. Mixed oxides as oxygen carries

There is always motivation in finding new alternative catalysts to enhance the chemical looping efficiency. In recent years, many researchers have been exploring the effect of the combination of various metals as a useful technique to improve the characteristics of oxygen carriers in terms of better catalytic activities, improved material mechanical strength, higher product selectivity, and minimizing carbon deposition (Jiao *et al* 2017). Mixed metal oxides have been studied extensively for their use in chemical looping technologies. Huang *et al* (2019) prepared mixed oxides by impregnating CuO and NiO on α-Al_2O_3 supports for chemical looping operation as given in figure 10 and observed that Ni–Cu–Al_2O_3 contains highly active redox-active lattice oxygen when compared to NiO or CuO.

Khzouz *et al* (2013) compared the activity of Cu-modified Ni/Al_2O_3 with pure Ni/Al_2O_3 and concluded that the tested Cu–Ni/Al_2O_3 presents higher H_2 selectivity and lower CO selectivity compared to Ni/Al_2O_3. Shamskar *et al* (2017) modified 25%Ni/Al_2O_3 by addition of 1%–5% Ce in a methane reforming reactor. Ce was chosen due to its great role in the stabilization of the alumina structure at high temperatures and the mobility of surface oxygen. Based on their results, the addition of Ce at a low amount, less than 2%, can increase the performance of the catalyst due to an improvement in the dispersion of Ni active sites with no sintering of active sites. In general, a combination of CeO_2 and Fe_2O_3 was suggested in the literature as a promising oxygen carrier for the CLR of methane. The formation Ce–Fe–O solid solution can improve the thermal stability and oxygen storage capacity of CeO_2, which is attributed to the formation of oxygen vacancies. This high cyclic stability in various reactions and high catalytic activity is explained by two reasons; the formation of Ce–Fe–O solid solution and strong interaction between Fe_2O_3 and CeO_2. It was reported that CuO modified Fe_2O_3 exhibits a less coke deposition of material due to partial coverage of CuO with a low propensity for coke formation while maintaining high hydrogen yields over many redox cycles.

Huang *et al* (2016) investigated the crystal structures of Ni–Fe oxygen carriers without inert components. As it can be seen from figure 11, the surface of fresh oxygen carrier particles is constituted of grains with sizes below 5 μm and indicates a good porosity, which is beneficial to the diffusion of gas molecules into the particles inner, increasing their reactivity. No important changes in the surface were detected after one cycle while after five cycles it can be observed that the particles surface is apparently worsened, and particle sizes grow to form agglomeration which means the thermal sintering appears on the oxygen carrier surface. The agglomeration is becoming more serious after ten cycles and the porosity disappears, and cracks appear due to the cumulative thermal stress.

3.8. Oxygen carriers with CO_2 sorbent

The steam reforming reaction releases hydrogen from the fuel, but also releases carbon in the form of CO_2. Steam methane reforming releases around 10–12 kg CO_2 for each kg of H_2 produced (Ozbilen *et al* 2013). SE-SMR unit is one of the intensified paths for the conversion of natural gas directly to high-purity hydrogen. This process combines the reforming reaction system in a single reactor with the addition of a high-temperature solid sorbent. The capture of CO_2 directly as it is produced, overcomes the equilibrium limitations of the WGS and reforming reactions and leads to remarkable improvement of the reactant conversion (Antzaras and Lemonidou 2022). Furthermore, enhanced hydrogen selectivity is attained in a single step, as a result of shifting the equilibrium of the overall reaction to the product side. Adding CO_2 capture to a steam methane reforming unit increases the cost of H_2 production by 32.5% and reduces net CO_2 emissions by 72%–83%. Since the cost of H_2 production is very sensitive to natural gas prices, its variation might greatly affect the costs of both H_2 production and CO_2 capture. It is critical to develop new materials which are capable of selectively capturing CO_2 under reaction conditions. There are three main categories of CO_2 sorbents including (a) low-temperature (less than 200 °C) material such as solid amine,

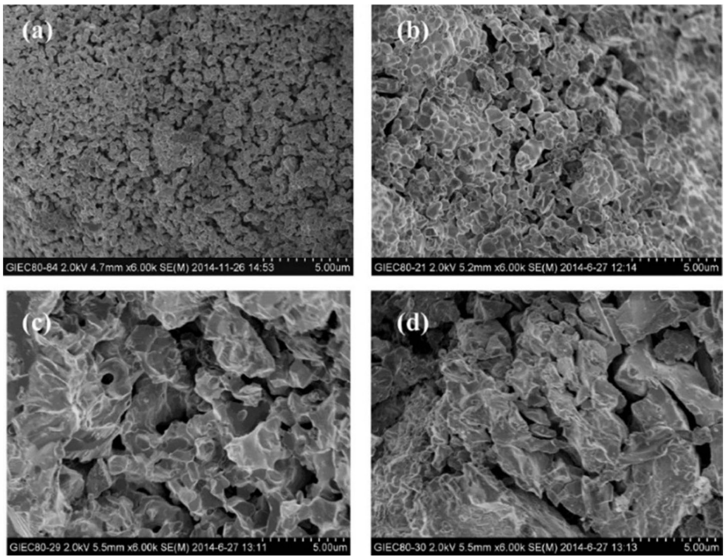

Figure 11. SEM images of the fresh and reacted oxygen carrier particles. (a) Fresh, (b) 1st cycle, (c) 5th cycle and (d) 10th cycle. Reprinted from Huang *et al*, Copyright (2016), with permission from Elsevier.

carbon, silica and zeolite-based materials; (b) intermediate-temperature (200 °C–450 °C) such as layered double hydroxide and MgO-based materials; and (c) high-temperature (450 °C–700 °C) sorbents such as alkaline metal-based and calcium-based materials (Antzaras and Lemonidou 2022). CaO, MgO and Li_2ZrO_3 are the most popular CO_2 sorbents in CLR units.

Alkaline-based sorbents such as alkaline silicates (Li_4SiO_4, $CaSiO_3$) or zirconates (Li_2ZrO_3, Na_2ZrO_3) have several advantages such as the high theoretical sorption capacity, the enhanced stability in multicycle operation and the relatively low temperatures required for regeneration (<750 °C) (Mendoza-Nieto *et al* 2018). Li_4SiO_4 sorbents have high CO_2 absorption capacity at temperatures of 600 °C–700 °C under high CO_2 concentration. However, they demonstrate inferior CO_2 capture properties when low CO_2 concentrations (10–20 vol%) are applied, indicating this kind of sorbents might not be an attractive candidate in sorption-enhanced reforming at CO_2 partial pressure below 0.15 bar due to the constraint on the external CO_2 diffusion to the surface of the particles. The incorporation of ions (Na, K, Ce, Mg, Ca) in the silicate structure can improve their performance at low CO_2 concentrations. In terms of sorption capacity, Li_4SiO_4 (8 mol CO_2 kg^{-1} sorbent) shows twice as much sorption capacity compared to Li_2ZrO_3 (4.5 mol CO_2 kg^{-1} sorbent) and Na_2ZrO_3 (3.5 mol CO_2 kg^{-1} sorbent).

Thanks to the advantages of CaO such as cheap price, fast carbonation kinetics, their wide availability and high theoretical sorption capacity (17 mol CO_2 kg^{-1} sorbent), CO_2 sorbents attracted much attention for high-temperature applications (Abanades and Alvarez 2003). Dou *et al* (2018) used a fixed-bed reactor to study the effect of CaO sorbent/NiO catalyst on product composition. They showed that the addition of the optimized amount of CaO-based sorbent in ethanol reforming has a positive effect on process performances and heat supply.

Decay in activity of CaO-based sorbents due to sintering during the calcination process was one of the limitations of this technology. The addition of steam during the carbonation step has also been reported to enhance the performance of CaO-based sorbents. One possible mechanism is based on the catalytic influence of steam, by which the production of surface –OH groups and bicarbonates may play an important role as intermediates and lead to enhanced carbonation of CaO.

Dolomite can be considered a promising CO_2 sorbent material, as it presents fast reaction rates, low cost and adequate stability compared to limestone. Magnesium oxides (MgO) are another attractive CO_2 sorbent due to their moderate CO_2 sorption capacity, wide availability, low price, highly reactive towards CO_2, and good CO_2 sorption capacity at 300 °C–450 °C and high pressure. Dang *et al* (2020) prepared porous microsphere Ni–CaO–MgO bifunctional material by hydrothermal method and tested it in a glycerol reforming system at 550 °C and S/C of 4. They showed that CaO–MgO had good CO_2 sorption performance. After ten cycles of sorption/desorption, the H_2 purity was more than 96%, showing excellent potential for promoting hydrogen production.

Martini *et al* (2021a) successfully demonstrated a sorption-enhanced steam reforming of methane at the TRL5 scale. Ca-based solid, Ni-catalyst and Cu-based material were used as CO_2 sorbent, reforming catalyst and oxygen carrier, respectively. It was found an increase in pressure negatively affects the sorption-enhanced reforming step by decreasing the purity of H_2 in the outlet stream. Furthermore, the average outlet H_2 fraction was not a strong function of the steam-to-carbon ratio. Increasing hydrogen fraction in the feed during the regeneration step from 20 vol% to 60 vol% resulted in an increase in the amount of regenerated sorbent from 53 wt% to 70 wt%. It was reported that after even 285 cycles, the solids were still chemically performing well, and the results were still reproducible. The same authors in another work (Martini *et al* 2021b) showed that a temperature range of 600 °C–650 °C was found to be the most appropriate for optimal performance of the sorption-enhanced reforming step. As temperature rises, carbonation and water gas shift reactions are relatively slow which leads to a significant CO exit fraction and a longer breakthrough period until the CaO sorbent is completely saturated. Furthermore, their experimental results revealed that a bed containing 27.5 wt% catalysts and 72.5 wt% sorbent is required for optimum reactor performance.

The major conclusions are drawn as follows:

- It is critical to select a suitable oxygen carrier based on its thermal stability to avoid material sintering.
- Toxicity and coke formation on the surface of Ni lead to blockage of nickel active sites and deactivation.
- In CLR processes, material deactivation caused by carbon deposition is one of the main issues.
- The oxygen carriers prepared by dry impregnation exhibit a lower tendency to increase the carbon deposition than the oxygen carriers prepared by a deposition-precipitation.
- SiO_2 and Al_2O_3 indicated excellent stability at high temperature.
- Among Ni, Co and Cu active metals, the highest glycerol conversion and the hydrogen selectivity were obtained by Ni/SiO_2 while Ni/Al_2O_3 catalyst exhibited the highest H_2/CO and the lowest CO/CO_2 ratio.
- By adding inert supports and using different preparation method, the performance of Cu-based material can be improved at high temperatures.
- The combination of various metal oxides is a useful technique to improve the characteristics of oxygen carriers in terms of catalytic activities, material mechanical strength, product selectivity, and minimizing carbon deposition.
- Among the possible metal oxides in CLR technology, cobalt shows the highest oxygen transport capability.
- Li_2ZrO_3 sorbents are attractive candidates at high CO_2 concentrations while CaO offer good performance for high-temperature application.

4. Thermodynamic analysis

The reduction of metal oxides at different temperatures is important to screen suitable oxygen carrier candidates and operational conditions in CLR. The selection of metal oxides can be made based on a modified Ellingham diagram, where the standard Gibbs free energy change variations with the temperature as shown in figure 12 (Fan *et al* 2015). A minimization of total Gibbs free energy is a suitable approach to determine the equilibrium compositions of any reacting system.

It can be observed that Mn is more easily oxidized compared to Fe and it is thermodynamically favorable for Mn to be oxidized by O_2 to MnO in temperatures up to 1600 °C (de Vos *et al* 2020a). The complete sequence in order of easiness of oxidation for all transition metals suitable for chemical looping can be ordered as follow Mn > Fe > Co > Ni > Cu. Metals that are more difficult to be oxidized compared to Cu are not suitable for chemical looping since they are not regenerable by air. The metals that are easier to be oxidized compared to Mn become too difficult to reduce with fuel.

Furthermore, the trend from Mn to Cu shows the suitability of the metal/metal oxide pairs for certain chemical looping technologies. While Fe/FeO is more viable for syngas generation by CLR, the transformation between CuO and Cu is utilized much more frequently for chemical looping combustion. As the Gibbs free energy for the oxidation of this Cu/CuO pair is almost zero, it is even eligible for chemical looping with oxygen uncoupling (de Vos *et al* 2020a).

Wang *et al* (2009) performed the thermodynamics study of glycerol reforming for syngas and H_2 generation. Through the Gibbs free energy minimization method, the optimum conditions were obtained at CO_2/glycerol ratios of 0–1 with reaction temperatures higher than 702 °C. Reaction at high pressure and CO_2 loading also gives a negative impact on the H_2 and syngas yields. Shah *et al* (2021) analyzed reforming of methane using $Ca_2Fe_2O_5$ as an oxygen carrier and showed that the change in Gibbs free energy for partial oxidation is much more negative in comparison to that of complete oxidation reaction, indicating partial oxidation of CH_4 using $Ca_2Fe_2O_5$ to form syngas is thermodynamically favored. At temperatures higher than 683 °C, CH_4 reacts with the oxygen carrier to form a limited amount of CO_2. It was found that the change in Gibbs free energy for partial oxidation of CH_4 using Fe_2O_3 was less negative compared to $Ca_2Fe_2O_5$, implying the thermodynamic superiority of the CaO-modified Fe_2O_3.

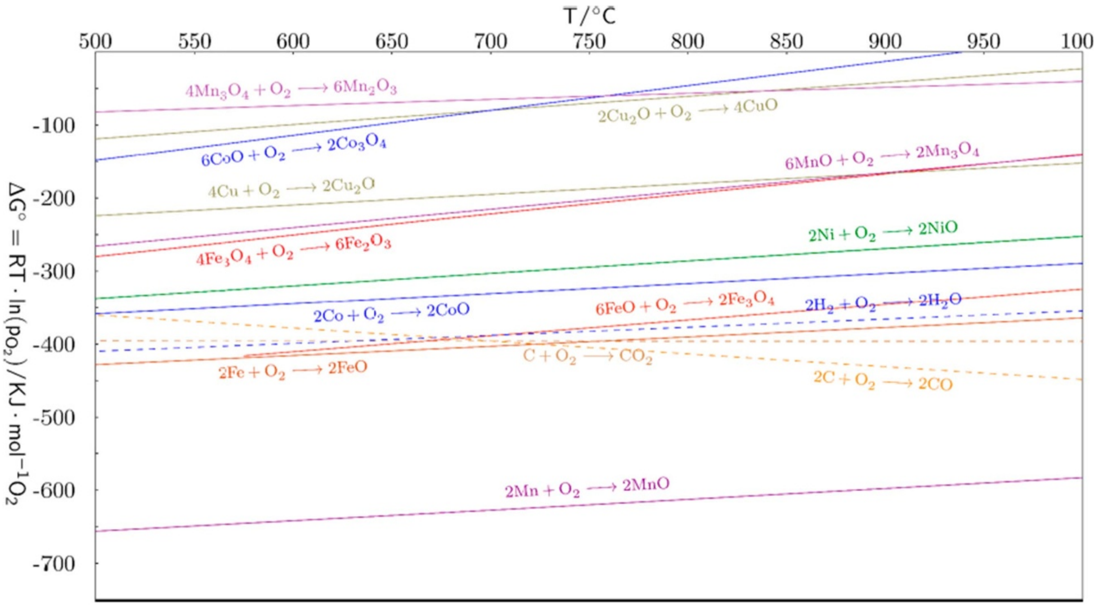

Figure 12. Ellingham diagram of different metal oxides. Reproduced from de Vos *et al* (2020a). CC BY 4.0.

5. Membrane-assisted CLR (MA-CLR)

The concept of a membrane-assisted chemical looping hybrid process to produce H_2 with high quality has been for the first time performed by the group of Gallucci (Gallucci *et al* 2008a, 2008b) and van Sint Annaland (Patil *et al* 2007). In this approach, the fuel reactor of the CLR process is coupled to H_2-permeated membranes. The combination of these two technologies has the potential of merging in an efficient way with direct CO_2 capture and pure H_2 production. Spallina *et al* (2016b) proposed a MA-CLR plant for pure H_2 production. In this system, methane is converted in the fuel reactor by reaction with steam and produces syngas. The oxygen carriers that act as a catalyst for both SMR and WGS reactions can be transported to the air reactor. The produced hydrogen is directly recovered from the fuel reactor via hydrogen-selective membranes immersed in this fluidized bed fuel reactor. The H_2 production efficiency of the MA-CLR was obtained to be more than 90%, which is 30% higher than conventional fired tubular reforming with CO_2 absorption technology based on MDEA solution. Medrano *et al* (2014) conducted a comparison between MA-CLR with conventional steam methane reforming coupled with chemical looping combustion, CLR and fluidized bed membrane reactor (FBMR). Their thermodynamic analysis has been carried out under different conditions such as reforming temperature, operating pressure and S/C ratio. As depicted in figure 13, compared to CLR, the main advantage is the possibility to obtain a high fuel conversion and thus a high performance at low temperatures due to the presence of the membranes. Furthermore, their investigation showed that at a lower temperature (600 °C–700 °C) the FBMR and the MA-CLR exhibit a reforming efficiency in the range of 75%–90% which is significantly higher than CLR and SMR. It FBMR and MA-CLR presented almost the same performance by increasing temperature. In another work, Medrano *et al* (2018) successfully demonstrated membrane-assisted methane reforming in which pure H_2 was separated from the fuel reactor through palladium-based membranes as shown in figure 13. Methane conversion above 90% was determined with the use of Ni-based catalyst as an oxygen carrier at 600 °C.

To achieve an economically viable chemical looping process, the cost of the oxygen carrier (and thus, at large scale production, especially the cost of the raw materials) is of vital importance (de Vos *et al* 2020a). Zhu *et al* (2018) assessed the techno-economic performance of a chemical looping plant employing different oxygen carriers. The corresponding levelized cost of electricity ranged from 75 to 89 \$ MWh^{-1}, in which nickel has the lowest levelized cost of electricity followed by copper. They showed that a rise in pressure from 6 bar to 18 bar initially decreased the cost of electricity from 105.3 to 74.5 \$ MWh^{-1}). Nazir *et al* (2018) evaluated a CLR plant integrated with a combined cycle power plant. The plant was operated at 18 bar and utilized a Ni-based material as oxygen carrier. The syngas produced in the CLR was subjected to water gas shift reaction before absorbing the CO_2 in a amine solution. A comprehensive sensitivity study indicated that the net electrical efficiencies ranged between 40% and 43.4% while the levelized cost of electricity varied between 132.7 and 145.9 \$ MWh^{-1}. Spallina *et al* (2016b) conducted a techno-economic assessment of a membrane-based CLR plant integrated with CO_2 capture. The operating pressure were in a range of

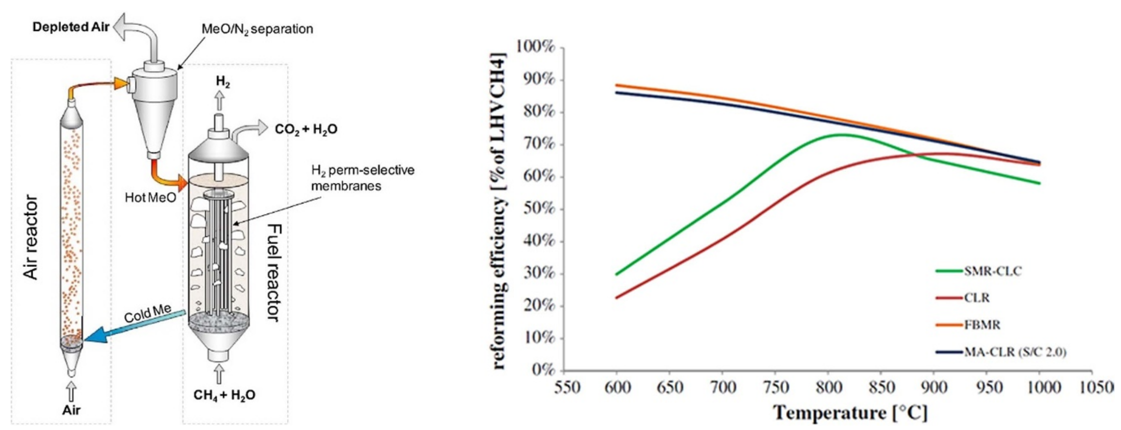

Figure 13. Schematic representation of MA-CLR system (left) and profile of reforming efficiency of the systems studied as a function of the reactor temperature (right). Reprinted from Medrano *et al*, Copyright (2014, 2018), with permission from Elsevier.

32–50 bar. Oxygen carrier reduction and methane reforming to syngas occur in the fuel reactor, while the produced hydrogen permeates through the membranes for separation. The plant exhibited low energy cost for CO_2 separation and compression which makes the overall reforming efficiency up to 20% higher than the conventional fired tubular reforming with CO_2 separation. Furthermore, the cost of hydrogen production decreased from 0.28 € $\text{Nm}_{\text{H2}}^{-3}$ to 0.19 € $\text{Nm}_{\text{H2}}^{-3}$. Spallina *et al* (2019) performed a full-scale techno-economic analysis of a chemical looping based process using dynamically operated packed bed reactors for the large-scale production of hydrogen (up to 30 000 $\text{Nm}^3\ \text{h}^{-1}$). Compared to a conventional H_2 production plant, the reforming efficiency was found to be 3% higher, while the required primary energy consumption to separate CO_2 was reported to be 0.47 MJLHV $\text{kg}_{\text{CO2}}^{-1}$ which is significantly lower than that of an amine-based plant (>1.35 MJLHV $\text{kg}_{\text{CO2}}^{-1}$). Moreover, I t was found that the cost of hydrogen production with the proposed process is 2.19 $ kg^{-1} with a CO_2 avoidance cost of 58.7 $ $\text{ton}_{\text{CO2}}^{-1}$ (compared to > 70.6 $ $\text{ton}_{\text{CO2}}^{-1}$ for solvent-based plant).

6. Conclusion

CLR is considered an emerging technology with the main advantage being the indirect contact of the fuel with the oxidant by means of an oxygen transfer material. In this work, the state-of-the-art oxygen carriers, and CO_2 sorbents in CLR of methane, ethanol and glycerol were summarized. The influence of key process variables controlling the CLR such as reactor temperature, pressure, water/fuel ratio and CO_2/fuel ratio on fuel conversion and syngas quality was assessed. The key messages of this work can be summarized as follows:

The methane conversion was found to be sensitive to the operating temperature below 800 °C.

- Co-feeding CO_2 into the fuel reactor was used to adjust the H_2/CO-ratio of the syngas, but a risk of coke formation in the bottom of the fuel reactor still exists.
- The high temperatures, high steam-to-glycerol ratios and low oxygen-to-glycerol ratios are feasible for glycerol reforming. In glycerol reforming, the temperature optimal is always somewhere around 650 °C–900 °C, while pressure is always kept low.
- The design and configuration of a reactor have an important role in product yield and process efficiency.
- From good heat and mass transfer behavior point of view, the fluidized bed reducer presents better performance compared to a moving bed or fixed bed reactor, while moving bed reactors offer better control over fuel utilization and conversions of the looping carrier.
- The development of the oxygen carrier with high selectivity, great stability, fast reactivity and resistance against carbon deposition are the key aspects of the successful operation of CLR.
- The preparation method of the catalyst plays a key role in the performance of the catalyst. The suitable and proper preparation method could give higher Ni dispersion on support, strong metal-support interaction, high catalytic activity, stability, and high resistance to carbon formation.
- Ce-based OCs are thermodynamically favored for preferentially oxidizing methane to syngas at low temperatures, but their redox stability and oxygen storage capacity need to be improved.
- Cu-based oxygen carriers are suitable for temperatures less than 1000 °C. They showed high oxygen transport capacity and high activity for complete oxidation of methane and strong resistance to carbon deposition.

- Ni is probably the best oxygen carrier for the steam reforming of glycerol. It offers high reactivity and stability during multi-redox cycles. However, carbon formation is easily generated on Ni-based oxygen carriers when carbon-containing fuels are used. Doping an impurity and adding a proportion of steam into the fuels can inhibit carbon formation.
- Type of catalyst support, mixed materials, using suitable catalyst preparation methods, the addition of promoters, modify particle size can be used to improve oxygen carrier characteristics.
- CaO-based solids and alkaline-based materials (Li_2ZrO_3, Li_4SiO_4, Na_2ZrO_3) are the most attractive CO_2 sorbent materials due to their application at relatively high temperatures.
- The SE-CLR concept has the potential to be considered an attractive technology for the production of hydrogen with H_2 purity of more than 98% and zero CO_2 emission.
- There are still challenges to be overcome in industrial applications, such as stabilizing the continuous long operation of the chemical looping process, controlling the proper heat balance between the oxidizer and reducer, and maintaining the recyclability properties of the oxygen carriers.

Data availability statement

The data that support the findings of this study are available upon reasonable request from the authors.

Acknowledgments

This project has received funding from the European Union's Horizon 2020 research and innovation program under Grant Agreement No. 884197 (GLAMOUR).

Conflict of interest

The authors have declared that no competing interests exist.

ORCID iDs

Rouzbeh Ramezani https://orcid.org/0000-0002-9234-4470
Luca Di Felice https://orcid.org/0000-0002-4378-6408
Fausto Gallucci https://orcid.org/0000-0001-6379-773X

References

Abad A, Adánez J, García-Labiano F, de Diego L F, Gayán P and Celaya J 2007 Mapping of the range of operational conditions for Cu-, Fe-, and Ni-based oxygen carriers in chemical-looping combustion *Chem. Eng. Sci.* **62** 533–49

Abanades J C and Alvarez D 2003 Conversion limits in the reaction of CO_2 with lime *Energy Fuels* **17** 308–15

Abdalazeez A, Wang W and Abuelgasim S 2021 Syngas production from chemical looping reforming of ethanol over iron-based oxygen carriers: theoretical analysis and experimental investigation *Chin. J. Chem. Eng.* **38** 123–31

Abuelgasim S, Wang W and Abdalazeez A 2021 A brief review for chemical looping combustion as a promising CO_2 capture technology: fundamentals and progress *Sci. Total Environ.* **764** 142892

Adanez J, Abad A, Garcia-Labiano F, Gayan P and de Diego L F 2012 Progress in chemical-looping combustion and reforming technologies *Prog. Energy Combust. Sci.* **38** 215–82

Adánez J, Abad A, Mendiara T, Gayán P, de Diego L F and García-Labiano F 2018 Chemical looping combustion of solid fuels *Prog. Energy Combust. Sci.* **65** 6–66

Adánez-Rubio I, Bararpour S T, Abad A, Gayán P, Williams G, Scullard A, Mahinpey N and Adánez J 2020 Performance evaluation of a Cu-based oxygen carrier impregnated onto ZrO_2 for chemical-looping combustion (CLC) *Ind. Eng. Chem. Res.* **59** 7255–66

Adánez-Rubio I, Ruiz J A C, García-Labiano F, de Diego L F and Adánez J 2021 Use of bio-glycerol for the production of synthesis gas by chemical looping reforming *Fuel* **288** 119578

Adhikari S, Fernando S and Haryanto A 2007 Production of hydrogen by steam reforming of glycerin over alumina-supported metal catalysts *Catal. Today* **129** 355–64

Alam S, Kumar J P, Rani K Y and Sumana C 2020 Comparative assessment of performances of different oxygen carriers in a chemical looping combustion coupled intensified reforming process through simulation study *J. Clean. Prod.* **262** 121146

Alirezaei I, Hafizi A and Rahimpour M R 2018 Syngas production in chemical looping reforming process over ZrO2 promoted Mn-based catalyst *J. CO2 Util.* **23** 105–16

Alirezaei I, Hafizi A, Rahimpour M R and Raeissi S 2016 Application of zirconium modified Cu-based oxygen carrier in chemical looping reforming *J. CO2 Util.* **14** 112–21

Antzara A, Heracleous E, Silvester L, Bukur D B and Lemonidou A A 2016 Activity study of NiO-based oxygen carriers in chemical looping steam methane reforming *Catal. Today* **272** 32–41

Antzaras A N and Lemonidou A A 2022 Recent advances on materials and processes for intensified production of blue hydrogen *Renew. Sustain. Energy Rev.* **155** 111917

Argyris P A, de Leeuwe C, Abbas S Z, Amieiro A, Poultson S, Wails D and Spallina V 2022 Chemical looping reforming for syngas generation at real process conditions in packed bed reactors: an experimental demonstration *Chem. Eng. J.* **435** 134883

Argyris P A, Wright A, Taheri Qazvini O and Spallina V 2022 Dynamic behaviour of integrated chemical looping process with pressure swing adsorption in small scale on-site H_2 and pure CO_2 production *Chem. Eng. J.* **428** 132606

Atilhan S, Park S, El-Halwagi M M, Atilhan M, Moore M and Nielsen R B 2021 Green hydrogen as an alternative fuel for the shipping industry *Curr. Opin. Chem. Eng.* **31** 100668

Ayodele B, Khan M R and Cheng C K 2016 Catalytic performance of ceria-supported cobalt catalyst for CO-rich hydrogen production from dry reforming of methane *Int. J. Hydrog. Energy* **41** 198–207

Bao J, Li Z and Cai N 2014 Interaction between iron-based oxygen carrier and four coal ashes during chemical looping combustion *Appl. Energy* **115** 549–58

Barreto L, Makihira A and Riahi K 2003 The hydrogen economy in the 21st century: a sustainable development scenario *Int. J. Hydrog. Energy* **28** 267–84

Baykara S Z 2018 Hydrogen: a brief overview on its sources, production and environmental impact *Int. J. Hydrog. Energy* **43** 10605–14

Byrd A J, Pant K K and Gupta R B 2008 Hydrogen production from glycerol by reforming in supercritical water over Ru/Al_2O_3 catalyst *Fuel* **87** 2956–60

Charisiou N D, Italiano C, Pino L, Sebastian V, Vita A and Goula M A 2020 Hydrogen production via steam reforming of glycerol over $Rh/\gamma\text{-}Al_2O_3$ catalysts modified with CeO_2, MgO or La_2O_3 *Renew. Energy* **162** 908–25

Chaubey R, Sahu S, James O O and Maity S 2013 A review on development of industrial processes and emerging techniques for production of hydrogen from renewable and sustainable sources *Renew. Sustain. Energy Rev.* **23** 443–62

Chein R-Y and Fung W-Y 2019 Syngas production via dry reforming of methane over CeO_2 modified Ni/Al_2O_3 catalysts *Int. J. Hydrog. Energy* **44** 14303–15

Chen H, Ding Y, Cong N T, Dou B, Dupont V, Ghadiri M and Williams P T 2011 A comparative study on hydrogen production from steam-glycerol reforming: thermodynamics and experimental *Renew. Energy* **36** 779–88

Chen J, Zhao K, Zhao Z, He F, Huang Z and Wei G 2019 Identifying the roles of MFe_2O_4 (M=Cu, Ba, Ni, and Co) in the chemical looping reforming of char, pyrolysis gas and tar resulting from biomass pyrolysis *Int. J. Hydrog. Energy* **44** 4674–87

Cheng Z, Qin L, Fan J A and Fan L-S 2018 New insight into the development of oxygen carrier materials for chemical looping systems *Engineering* **4** 343–51

Cheng Z, Zhang L, Jin N, Zhu Y, Chen L, Yang Q, Yan M, Ma X and Wang X 2021 Effect of calcination temperature on the performance of hexaaluminate supported CeO_2 for chemical looping dry reforming *Fuel Process. Technol.* **218** 106873

Chiron F-X and Patience G S 2012 Kinetics of mixed copper–iron based oxygen carriers for hydrogen production by chemical looping water splitting *Int. J. Hydrog. Energy* **37** 10526–38

Dai X P, Li J, Fan J T, Wei W S and Xu J 2012 Synthesis gas generation by chemical-looping reforming in a circulating fluidized bed reactor using Perovskite LaFeO 3-based oxygen carriers *Ind. Eng. Chem. Res.* **51** 11072–82

Dang C, Liu L, Yang G, Cai W, Long J and Yu H 2020 Mg-promoted Ni-CaO microsphere as bi-functional catalyst for hydrogen production from sorption-enhanced steam reforming of glycerol *Chem. Eng. J.* **383** 123204

de Diego L F, Ortiz M, García-Labiano F, Adánez J, Abad A and Gayán P 2009 Hydrogen production by chemical-looping reforming in a circulating fluidized bed reactor using Ni-based oxygen carriers *J. Power Sources* **192** 27–34

de Vos Y, Jacobs M, van der Voort P, van Driessche I, Snijkers F and Verberckmoes A 2020a Development of stable oxygen carrier materials for chemical looping processes—a review *Catalysts* **10** 926

Delparish A and Avci A K 2016 Intensified catalytic reactors for Fischer-Tropsch synthesis and for reforming of renewable fuels to hydrogen and synthesis gas *Fuel Process. Technol.* **151** 72–100

Delparish A, Koc S, Caglayan B S and Avci A K 2019 Oxidative steam reforming of glycerol to synthesis gas in a microchannel reactor *Catal. Today* **323** 200–8

Ding H, Luo C, Li X, Cao D, Shen Q and Zhang L 2019 Development of BaSrCo-based perovskite for chemical-looping steam methane reforming: a study on synergistic effects of A-site elements and CeO_2 support *Fuel* **253** 311–9

Dou B, Dupont V, Rickett G, Blakeman N, Williams P T, Chen H, Ding Y and Ghadiri M 2009 Hydrogen production by sorption-enhanced steam reforming of glycerol *Bioresour. Technol.* **100** 3540–7

Dou B, Song Y, Wang C, Chen H, Yang M and Xu Y 2014 Hydrogen production by enhanced-sorption chemical looping steam reforming of glycerol in moving-bed reactors *Appl. Energy* **130** 342–9

Dou B, Zhang H, Cui G, Wang Z, Jiang B, Wang K, Chen H and Xu Y 2017 Hydrogen production and reduction of Ni-based oxygen carriers during chemical looping steam reforming of ethanol in a fixed-bed reactor *Int. J. Hydrog. Energy* **42** 26217–30

Dou B, Zhang H, Cui G, Wang Z, Jiang B, Wang K, Chen H and Xu Y 2018 Hydrogen production by sorption-enhanced chemical looping steam reforming of ethanol in an alternating fixed-bed reactor: sorbent to catalyst ratio dependencies *Energy Convers. Manage.* **155** 243–52

Elias K F M, Lucrédio A F and Assaf E M 2013 Effect of CaO addition on acid properties of $Ni–Ca/Al_2O_3$ catalysts applied to ethanol steam reforming *Int. J. Hydrog. Energy* **38** 4407–17

Fan L-S, Zeng L and Luo S 2015 Chemical-looping technology platform *AIChE J.* **61** 2–22

Fan L-S, Zeng L, Wang W and Luo S 2012 Chemical looping processes for CO_2 capture and carbonaceous fuel conversion—prospect and opportunity *Energy Environ. Sci.* **5** 7254–80

Forero C R, Gayán P, García-Labiano F, de Diego L F, Abad A and Adánez J 2010 Effect of gas composition in chemical-looping combustion with copper-based oxygen carriers: fate of sulphur *Int. J. Greenh. Gas Control* **4** 762–70

Forero C R, Gayán P, García-Labiano F, de Diego L F, Abad A and Adánez J 2011 High temperature behaviour of a $CuO/\gamma Al_2O_3$ oxygen carrier for chemical-looping combustion *Int. J. Greenh. Gas Control* **5** 659–67

Forutan H R, Karimi E, Hafizi A, Rahimpour M R and Keshavarz P 2015 Expert representation chemical looping reforming: a comparative study of Fe, Mn, Co and Cu as oxygen carriers supported on Al_2O_3 *J. Ind. Eng. Chem.* **21** 900–11

Gallucci F, van Sint Annaland M and Kuipers J A M 2008a Autothermal reforming of methane with integrated CO_2 capture in a novel fluidized bed membrane reactor. Part 1: experimental demonstration *Top. Catal.* **51** 133–45

Gallucci F, van Sint Annaland M and Kuipers J A M 2008b Autothermal reforming of methane with integrated CO_2 capture in a novel fluidized bed membrane reactor. Part 2 comparison of reactor configurations *Top. Catal.* **51** 146–57

García-Díez E, García-Labiano F, de Diego L F, Abad A, Gayán P and Adánez J 2017 Autothermal chemical looping reforming process of different fossil liquid fuels *Int. J. Hydrog. Energy* **42** 13633–40

García-García F R and Metcalfe I S 2021 Chemical looping dry reforming of methane using mixed oxides of iron and cerium: operation window *Catal. Commun.* **160** 106356

Garcia-Labiano F, de Diego L F, Garcia-Diez E, Serrano A, Abad A, Gayan P and Adanez J 2014 Combustion and reforming of ethanol in a chemical looping continuous unit *Energy Proc.* **63** 53–62

García-Labiano F, García-Díez E, de Diego L F, Serrano A, Abad A, Gayán P, Adánez J and Ruíz J A C 2015a Syngas/H2 production from bioethanol in a continuous chemical-looping reforming prototype *Fuel Process. Technol.* **137** 24–30

Guerrero-Caballero J, Kane T, Haidar N, Jalowiecki-Duhamel L and Löfberg A 2019 Ni, Co, Fe supported on Ceria and Zr doped Ceria as oxygen carriers for chemical looping dry reforming of methane *Catal. Today* **333** 251–8

Guo L, Zhao H and Zheng C 2015 Synthesis gas generation by chemical-looping reforming of biomass with natural copper ore as oxygen carrier *Waste Biomass Valorization* **6** 81–89

Guo M, Cheng Z, Liu Y, Qin L, Goetze J, Fan J A and Fan L-S 2020 Cobalt doping modification for enhanced methane conversion at low temperature in chemical looping reforming systems *Catal. Today* **350** 156–64

Hafizi A, Rahimpour M R and Hassanajili S 2016 High purity hydrogen production via sorption enhanced chemical looping reforming: application of 22Fe_2O_3/$MgAl_2O_4$ and 22Fe_2O_3/Al_2O_3 as oxygen carriers and cerium promoted CaO as CO_2 sorbent *Appl. Energy* **169** 629–41

Han Y *et al* 2022 Highly active and anticoke Ni/CeO_2 with ultralow Ni loading in chemical looping dry reforming via the strong metal−support interaction *ACS Sustain. Chem. Eng.* **23** 29

Hassani Rad S J, Haghighi M, Alizadeh Eslami A, Rahmani F and Rahemi N 2016 Sol–gel vs. impregnation preparation of MgO and CeO_2 doped Ni/Al_2O_3 nanocatalysts used in dry reforming of methane: effect of process conditions, synthesis method and support composition *Int. J. Hydrog. Energy* **41** 5335–50

Hossain M M and de Lasa H I 2008 Chemical-looping combustion (CLC) for inherent CO_2 separations—a review *Chem. Eng. Sci.* **63** 4433–51

Hu G, Nicholas N J, Smith K H, Mumford K A, Kentish S E and Stevens G W 2016 Carbon dioxide absorption into promoted potassium carbonate solutions: a review *Int. J. Greenh. Gas Control* **53** 28–40

Hu J, Chen S and Xiang W 2021a Ni, Co and Cu-promoted iron-based oxygen carriers in methane-fueled chemical looping hydrogen generation process *Fuel Process. Technol.* **221** 106917

Hu J, Zhang T, Zhang Q, Yan X, Zhao S, Dang J and Wang W 2021b Application of calcium oxide/ferric oxide composite oxygen carrier for corn straw chemical looping gasification *Bioresour. Technol.* **330** 125011

Hu Z, Miao Z, Wu J and Jiang E 2021c Nickel-iron modified natural ore oxygen carriers for chemical looping steam methane reforming to produce hydrogen *Int. J. Hydrog. Energy* **46** 39700–18

Huang J, Liu W, Hu W, Metcalfe I, Yang Y and Liu B 2019 Phase interactions in Ni-Cu-Al_2O_3 mixed oxide oxygen carriers for chemical looping applications *Appl. Energy* **236** 635–47

Huang J, Liu W, Yang Y and Liu B 2018 High-performance Ni-Fe Redox catalysts for selective CH_4 to syngas conversion via chemical looping *ACS Catal.* **8** 1748–56

Huang Z, Jiang H, He F, Chen D, Wei G, Zhao K, Zheng A, Feng Y, Zhao Z and Li H 2016 Evaluation of multi-cycle performance of chemical looping dry reforming using CO_2 as an oxidant with Fe–Ni bimetallic oxides *J. Energy Chem.* **25** 62–70

Iglesias I, Baronetti G and Mariño F 2017 Ni/$Ce_{0.95}M_{0.05}O_{2-d}$ (M = Zr, Pr, La) for methane steam reforming at mild conditions *Int. J. Hydrog. Energy* **42** 29735–44

Iliuta I and Iliuta M C 2013 Biosyngas production in an integrated aqueous-phase glycerol reforming/chemical looping combustion process *Ind. Eng. Chem. Res.* **52** 16142–61

Imtiaz Q, Yüzbasi N S, Abdala P M, Kierzkowska A M, van Beek W, Broda M and Müller C R 2015 Development of $MgAl_2O_4$-stabilized, Cu-doped, Fe_2O_3-based oxygen carriers for thermochemical water-splitting *J. Mater. Chem.* A **4** 113–23

Iriondo A, Barrio V L, Cambra J F, Arias P L, Güemez M B, Navarro R M, Sánchez-Sánchez M C and Fierro J L G 2008 Hydrogen production from glycerol over nickel catalysts supported on Al_2O_3 modified by Mg, Zr, Ce or La *Top. Catal.* **49** 46–58

Isarapakdeetham S, Kim-Lohsoontorn P, Wongsakulphasatch S, Kiatkittipong W, Laosiripojana N, Gong J and Assabumrungrat S 2020 Hydrogen production via chemical looping steam reforming of ethanol by Ni-based oxygen carriers supported on CeO_2 and La_2O_3 promoted Al_2O_3 *Int. J. Hydrog. Energy* **45** 1477–91

Jang J T, Yoon K J, Bae J W and Han G Y 2014 Cyclic production of syngas and hydrogen through methane-reforming and water-splitting by using ceria–zirconia solid solutions in a solar volumetric receiver–reactor *Sol. Energy* **109** 70–81

Jerndal E, Mattisson T and Lyngfelt A 2006 Thermal analysis of chemical-looping combustion *Chem. Eng. Res. Des.* **84** 795–806

Ji M and Wang J 2021 Review and comparison of various hydrogen production methods based on costs and life cycle impact assessment indicators *Int. J. Hydrog. Energy* **46** 38612–35

Jiang B, Dou B, Song Y, Zhang C, Du B, Chen H, Wang C and Xu Y 2015 Hydrogen production from chemical looping steam reforming of glycerol by Ni-based oxygen carrier in a fixed-bed reactor *Chem. Eng. J.* **280** 459–67

Jiang B, Dou B, Wang K, Zhang C, Song Y, Chen H and Xu Y 2016 Hydrogen production by chemical looping steam reforming of ethanol using NiO/montmorillonite oxygen carriers in a fixed-bed reactor *Chem. Eng. J.* **298** 96–106

Jiang B, Li L, Bian Z, Li Z, Othman M, Sun Z, Tang D, Kawi S and Dou B 2018a Hydrogen generation from chemical looping reforming of glycerol by Ce-doped nickel phyllosilicate nanotube oxygen carriers *Fuel* **222** 185–92

Jiang B, Li L, Bian Z, Li Z, Sun Y, Sun Z, Tang D, Kawi S, Dou B and Goula M A 2018b Chemical looping glycerol reforming for hydrogen production by Ni@ZrO_2 nanocomposite oxygen carriers *Int. J. Hydrog. Energy* **43** 13200–11

Jiang B, Li L, Zhang Q, Ma J, Zhang H, Bai J, Bian Z, Dou B, Kawi S and Tang D 2020 Chemical looping reforming of glycerol for continuous H_2 Production by moving-bed reactors: simulation and experiment *Energy Fuels* **34** 1841–50

Jiao Y, He Z, Wang J and Chen Y 2017 n-decane steam reforming for hydrogen production over mono- and bi-metallic Co-Ni/Ce-Al_2O_3 catalysts: structure-activity correlations *Energy Convers. Manage.* **148** 954–62

Johansson M, Mattisson T and Lyngfelt A 2006 Investigation of Mn_3O_4 with stabilized ZrO_2 for chemical-looping combustion *Chem. Eng. Res. Des.* **84** 807–18

Johansson M, Mattisson T, Lyngfelt A and Abad A 2008 Using continuous and pulse experiments to compare two promising nickel-based oxygen carriers for use in chemical-looping technologies *Fuel* **87** 988–1001

Kang D, Lim H S, Lee M and Lee J W 2018 Syngas production on a Ni-enhanced Fe_2O_3/Al_2O_3 oxygen carrier via chemical looping partial oxidation with dry reforming of methane *Appl. Energy* **211** 174–86

Kang Y, Tian M, Huang C, Lin J, Hou B, Pan X, Li L, Rykov A I, Wang J and Wang X 2019 Improving syngas selectivity of Fe_2O_3/Al_2O_3 with yttrium modification in chemical looping methane conversion *ACS Catal.* **9** 8373–82

Keller M, Fung J, Leion H and Mattisson T 2016 Cu-impregnated alumina/silica bed materials for chemical looping reforming of biomass gasification gas *Fuel* **180** 448–56

Khajenoori M, Rezaei M and Meshkani F 2015 Dry reforming over CeO_2-promoted Ni/MgO nano-catalyst: effect of Ni loading and CH_4/CO_2 molar ratio *J. Ind. Eng. Chem.* **21** 717–22

Khzouz M, Wood J, Pollet B and Bujalski W 2013 Characterization and activity test of commercial Ni/Al_2O_3, $Cu/ZnO/Al_2O_3$ and prepared Ni–Cu/Al_2O_3 catalysts for hydrogen production from methane and methanol fuels *Int. J. Hydrog. Energy* **38** 1664–75

Lee D, Nam H, Kim H, Hwang B, Baek J-I and Ryu H-J 2021 Experimental screening of oxygen carrier for a pressurized chemical looping combustion *Fuel Process. Technol.* **218** 106860

Li D, Li K, Xu R, Zhu X, Wei Y, Tian D, Cheng X and Wang H 2019a Enhanced CH_4 and CO oxidation over Ce1- xFexO_2- hybrid catalysts by tuning the lattice distortion and the state of surface iron species *ACS Appl. Mater. Interfaces* **11** 19227–41

Li D, Xu R, Jia Y, Ning P and Li K 2019b Controlled synthesis of α-Fe_2O_3 hollows from β-FeOOH rods *Chem. Phys. Lett.* **731** 136623

Li D, Xu S, Song K, Chen C, Zhan Y and Jiang L 2018a Hydrotalcite-derived Co/Mg(Al)O as a stable and coke-resistant catalyst for low-temperature carbon dioxide reforming of methane *Appl. Catal.* A **552** 21–29

Li L, Jiang B, Tang D, Zheng Z and Zhao C 2018b Hydrogen production from chemical looping reforming of ethanol using Ni/CeO_2 nanorod oxygen carrier *Catalysts* **8** 257

Li L, Song Y, Jiang B, Wang K and Zhang Q 2017 A novel oxygen carrier for chemical looping reforming: $laNiO_3$ perovskite supported on montmorillonite *Energy* **131** 58–66

Li T, Wu Q, Wang W, Xiao Y P, Liu C and Yang F 2020 Solid-solid reaction of $CuFe_2O_4$ with C in chemical looping system: a comprehensive study *Fuel* **267** 117163

Lind F, Israelsson M, Seemann M and Thunman H 2012 Manganese oxide as catalyst for tar cleaning of biomass-derived gas *Biomass Convers. Biorefin.* **2** 133–40

Long Y *et al* 2020 Ce-Fe-Zr-O/MgO coated monolithic oxygen carriers for chemical looping reforming of methane to co-produce syngas and H_2 *Chem. Eng. J.* **388** 124190

López Ortiz A, Meléndez Zaragoza M and Collins-Martínez V 2015 Thermodynamic analysis of the ethanol chemical looping autothermal reforming with CO_2 capture *Int. J. Hydrog. Energy* **40** 17180–91

Lu C, Xu R, Muhammad I K, Zhu X, Wei Y, Qi X and Li K 2021 Thermodynamic evolution of magnetite oxygen carrier via chemical looping reforming of methane *J. Nat. Gas Eng.* **85** 103704

Luo C, Dou B, Zhang H, Zhao L, Zeng P, Gao D, Wang Y, Chen H and Xu Y 2022 Hydrogen and syngas co-production by coupling of chemical looping water splitting and glycerol oxidation reforming using Ce–Ni modified Fe-based oxygen carriers *J. Clean. Prod.* **335** 130299

Ma Z, Zhang S and Lu Y 2020 Activation mechanism of Fe_2O_3-Al_2O_3 oxygen carrier in chemical looping combustion *Energy Fuels* **34** 16350–5

Martini M, Druiff M, van Sint Annaland M and Gallucci F 2021a Experimental demonstration of the Ca-Cu looping process *Chem. Eng. J.* **418** 129505

Martini M, Jain S, Gallucci F and van Sint Annaland M 2021b Model validation of the Ca-Cu looping process *Chem. Eng. J.* **410** 128351

Masoudi Soltani S, Lahiri A, Bahzad H, Clough P, Gorbounov M and Yan Y 2021 Sorption-enhanced steam methane reforming for combined CO_2 capture and hydrogen production: a state-of-the-art review *Carbon Capture Sci. Technol.* **1** 100003

Medrano J A, Potdar I, Melendez J, Spallina V, Pacheco-Tanaka D A, van Sint Annaland M and Gallucci F 2018 The membrane-assisted chemical looping reforming concept for efficient H_2 production with inherent CO_2 capture: experimental demonstration and model validation *Appl. Energy* **215** 75–86

Medrano J A, Spallina V, van Sint Annaland M and Gallucci F 2014 Thermodynamic analysis of a membrane-assisted chemical looping reforming reactor concept for combined H_2 production and CO_2 capture *Int. J. Hydrog. Energy* **39** 4725–38

Mendoza-Nieto J A, Duan Y and Pfeiffer H 2018 Alkaline zirconates as effective materials for hydrogen production through consecutive carbon dioxide capture and conversion in methane dry reforming *Appl. Catal.* B **238** 576–85

Meshksar M, Daneshmand-Jahromi S and Rahimpour M R 2017 Synthesis and characterization of cerium promoted Ni/SBA-16 oxygen carrier in cyclic chemical looping steam methane reforming *J. Taiwan Inst. Chem. Eng.* **76** 73–82

Nadgouda S G, Guo M, Tong A and Fan L-S 2019 High purity syngas and hydrogen coproduction using copper-iron oxygen carriers in chemical looping reforming process *Appl. Energy* **235** 1415–26

Nandy A, Loha C, Gu S, Sarkar P, Karmakar M K and Chatterjee P K 2016 Present status and overview of chemical looping combustion technology *Renew. Sustain. Energy Rev.* **59** 597–619

Nazari M, Soltanieh M, Heydarinasab A and Maddah B 2021 Synthesis of a new self-supported Mgy(CuxNi0.6-xMn0.4)1-yFe_2O_4 oxygen carrier for chemical looping steam methane reforming process *Int. J. Hydrog. Energy* **46** 19397–420

Nazir S M, Morgado J F, Bolland O, Quinta-Ferreira R and Amini S 2018 Techno-economic assessment of chemical looping reforming of natural gas for hydrogen production and power generation with integrated CO_2 capture *Int. J. Greenh. Gas Control* **78** 7–20

Neal L, Shafiefarhood A and Li F 2015 Effect of core and shell compositions on MeO_x@$La_ySr_{1-y}FeO_3$ core–shell redox catalysts for chemical looping reforming of methane *Appl. Energy* **157** 391–8

Ni Y, Wang C, Chen Y, Cai X, Dou B, Chen H, Xu Y, Jiang B and Wang K 2017 High purity hydrogen production from sorption enhanced chemical looping glycerol reforming: application of NiO-based oxygen transfer materials and potassium promoted Li_2ZrO_3 as CO_2 sorbent *Appl. Therm. Eng.* **124** 454–65

Nieva M A, Villaverde M M, Monzón A, Garetto T F and Marchi A J 2014 Steam-methane reforming at low temperature on nickel-based catalysts *Chem. Eng. J.* **235** 158–66

Nikoo M K and Amin N A S 2011 Thermodynamic analysis of carbon dioxide reforming of methane in view of solid carbon formation *Fuel Process. Technol.* **92** 678–91

Nimmas T, Wongsakulphasatch S, Kui Cheng C and Assabumrungrat S 2020 Bi-metallic CuO-NiO based multifunctional material for hydrogen production from sorption-enhanced chemical looping autothermal reforming of ethanol *Chem. Eng. J.* **398** 125543

Osman M, Khan M N, Zaabout A, Cloete S and Amini S 2021 Review of pressurized chemical looping processes for power generation and chemical production with integrated CO_2 capture *Fuel Process. Technol.* **214** 106684

Ozbilen A, Dincer I and Rosen M A 2013 Comparative environmental impact and efficiency assessment of selected hydrogen production methods *Environ. Impact. Assess. Rev.* **42** 1–9

Pantaleo G, la Parola V, Deganello F, Calatozzo P, Bal R and Venezia A M 2015 Synthesis and support composition effects on CH_4 partial oxidation over Ni–CeLa oxides *Appl. Catal.* B **164** 135–43

Papageridis K N, Siakavelas G, Charisiou N D, Avraam D G, Tzounis L, Kousi K and Goula M A 2016 Comparative study of Ni, Co, Cu supported on γ-alumina catalysts for hydrogen production via the glycerol steam reforming reaction *Fuel Process. Technol.* **152** 156–75

Papageridis K N, Siakavelas G, Charisiou N D and Goula M A 2015 Effect of the active metal supported on SiO_2 to the selective hydrogen production on the glycerol steam reforming reaction *3rd Int. Conf. on Sustainable Solid Waste Management (TINOS 2015)* (*Tinos Island, Cyclades, Greece*)

Patcharavorachot Y, Chatrattanawet N, Arpornwichanop A and Assabumrungrat S 2019 Optimization of hydrogen production from three reforming approaches of glycerol via using supercritical water with *in situ* CO_2 separation *Int. J. Hydrog. Energy* **44** 2128–40

Patil C S, van Sint Annaland M and Kuipers J A M 2007 Fluidised bed membrane reactor for ultrapure hydrogen production via methane steam reforming: experimental demonstration and model validation *Chem. Eng. Sci.* **62** 2989–3007

Porrazzo R, White G and Ocone R 2014 Aspen plus simulations of fluidised beds for chemical looping combustion *Fuel* **136** 46–56

Qin L, Guo M, Liu Y, Cheng Z, Fan J A and Fan L-S 2018 Enhanced methane conversion in chemical looping partial oxidation systems using a copper doping modification *Appl. Catal.* B **235** 143–9

Qingli X, Zhengdong Z, Kai H, Shanzhi X, Chuang M, Chenge C, Huan Y, Yang Y and Yongjie Y 2021 Ni supported on MgO modified attapulgite as catalysts for hydrogen production from glycerol steam reforming *Int. J. Hydrog. Energy* **46** 27380–93

Roslan N A, Abidin S Z, Ideris A and Vo D-V N 2020 A review on glycerol reforming processes over Ni-based catalyst for hydrogen and syngas productions *Int. J. Hydrog. Energy* **45** 18466–89

Rydén M, Lyngfelt A and Mattisson T 2008 Chemical-looping combustion and chemical-looping reforming in a circulating fluidized-bed reactor using Ni-based oxygen carriers *Energy Fuels* **22** 2585–97

Rydén M, Lyngfelt A and Mattisson T 2011 $CaMn_{0.875}Ti_{0.125}O_3$ as oxygen carrier for chemical-looping combustion with oxygen uncoupling (CLOU)—experiments in a continuously operating fluidized-bed reactor system *Int. J. Greenh. Gas Control* **5** 356–66

Sahraei O A, Desgagnés A, Larachi F and Iliuta M C 2021 A comparative study on the performance of M (Rh, Ru, Ni)-promoted metallurgical waste driven catalysts for H_2 production by glycerol steam reforming *Int. J. Hydrog. Energy* **46** 32017–35

Sastre D, Galván C Á, Pizarro P and Coronado J M 2022 Enhanced performance of CH_4 dry reforming over $La_{0.9}Sr_{0.1}FeO_3$/YSZ under chemical looping conditions *Fuel* **309** 122122

Sastre D, Serrano D P, Pizarro P and Coronado J M 2019 Chemical insights on the activity of $La_{1-x}Sr_xFeO_3$ perovskites for chemical looping reforming of methane coupled with CO_2-splitting *J. CO2 Util.* **31** 16–26

Saupsor J, Kasempremchit N, Bumroongsakulsawat P, Kim-Lohsoontorn P, Wongsakulphasatch S, Kiatkittipong W, Laosiripojana N, Gong J and Assabumrungrat S 2020 Performance comparison among different multifunctional reactors operated under energy self-sufficiency for sustainable hydrogen production from ethanol *Int. J. Hydrog. Energy* **45** 18309–20

Saupsor J, Pei C, Li H, Wongsakulphasatch S, Kim-Lohsoontorn P, Ratchahat S, Kiatkittipong W, Assabumrungrat S and Gong J 2021 Bifunctional catalyst NiFe-MgAl for hydrogen production from chemical looping ethanol reforming *Energy Fuels* **35** 11580–92

Senseni A Z, Meshkani F, Seyed Fattahi S M and Rezaei M 2017 A theoretical and experimental study of glycerol steam reforming over $Rh/MgAl_2O_4$ catalysts *Energy Convers. Manage.* **154** 127–37

Shah V, Cheng Z, Baser D S, Fan J A and Fan L-S 2021 Highly selective production of syngas from chemical looping reforming of methane with CO_2 utilization on MgO-supported calcium ferrite redox materials *Appl. Energy* **282** 116111

Shamskar F R, Meshkani F and Rezaei M 2017 Preparation and characterization of ultrasound-assisted co-precipitated nanocrystalline La-, Ce-, Zr- promoted $Ni-Al_2O_3$ catalysts for dry reforming reaction *J. CO2 Util.* **22** 124–34

Siriwardane R, Tian H and Fisher J 2015 Production of pure hydrogen and synthesis gas with Cu–Fe oxygen carriers using combined processes of chemical looping combustion and methane decomposition/reforming *Int. J. Hydrog. Energy* **40** 1698–708

Solunke R D and Veser G 2010 Hydrogen production via chemical looping steam reforming in a periodically operated fixed-bed reactor *Ind. Eng. Chem. Res.* **49** 11037–44

Spallina V, Gallucci F, Romano M C and van Sint Annaland M 2016a Pre-combustion packed bed chemical looping (PCCL) technology for efficient H_2-rich gas production processes *Chem. Eng. J.* **294** 478–94

Spallina V, Marinello B, Gallucci F, Romano M C and van Sint Annaland M 2017 Chemical looping reforming in packed-bed reactors: modelling, experimental validation and large-scale reactor design *Fuel Process. Technol.* **156** 156–70

Spallina V, Motamedi G, Gallucci F and van Sint Annaland M 2019 Techno-economic assessment of an integrated high pressure chemical-looping process with packed-bed reactors in large scale hydrogen and methanol production *Int. J. Greenh. Gas Control* **88** 71–84

Spallina V, Pandolfo D, Battistella A, Romano M C, van Sint Annaland M and Gallucci F 2016b Techno-economic assessment of membrane assisted fluidized bed reactors for pure H_2 production with CO_2 capture *Energy Convers. Manage.* **120** 257–73

Suero S R, Cano B L, Álvarez-Murillo A, Al-Kassir A and Yusaf T 2015 Glycerin, a biodiesel by-product with potentiality to produce hydrogen by steam gasification *Energies* **8** 12765–75

Sun Y, Li J and Li H 2022 Core-shell-like Fe_2O_3/MgO oxygen carriers matched with fluidized bed reactor for chemical looping reforming *Chem. Eng. J.* **431** 134173

Sun Z, Lu D Y, Symonds R T and Hughes R W 2020 Chemical looping reforming of CH_4 in the presence of CO_2 using ilmenite ore and NiO-modified ilmenite ore oxygen carriers *Chem. Eng. J.* **401** 123481

Svoboda K, Siewiorek A, Baxter D, Rogut J and Pohořelý M 2008 Thermodynamic possibilities and constraints for pure hydrogen production by a nickel and cobalt-based chemical looping process at lower temperatures *Energy Convers. Manage.* **49** 221–31

Tang M, Xu L and Fan M 2015 Progress in oxygen carrier development of methane-based chemical-looping reforming: a review *Appl. Energy* **151** 143–56

Tavanarad M, Rezaei M and Meshkani F 2021 Preparation and evaluation of $Ni/\gamma-Al_2O_3$ catalysts promoted by alkaline earth metals in glycerol reforming with carbon dioxide *Int. J. Hydrog. Energy* **46** 24991–5003

Teh L P, Setiabudi H D, Timmiati S N, Aziz M A A, Annuar N H R and Ruslan N N 2021 Recent progress in ceria-based catalysts for the dry reforming of methane: a review *Chem. Eng. Sci.* **242** 116606

Tian X, Su M and Zhao H 2020 Kinetics of redox reactions of $CuO@TiO_2–Al_2O_3$ for chemical looping combustion and chemical looping with oxygen uncoupling *Combust. Flame* **213** 255–67

Trevisanut C, Mari M, Millet J M and Cavani F 2015 Chemical-loop reforming of ethanol over metal ferrites: an analysis of structural features affecting reactivity *Int. J. Hydrog. Energy* **40** 5264–71

Usman M, Wan Daud W M A and Abbas H F 2015 Dry reforming of methane: influence of process parameters—a review *Renew. Sustain. Energy Rev.* **45** 710–44

van Renssen S 2020 The hydrogen solution? *Nat. Clim. Change* **10** 799–801

Vizcaíno A J, Arena P, Baronetti G, Carrero A, Calles J A, Laborde M A and Amadeo N 2008 Ethanol steam reforming on Ni/Al_2O3 catalysts: effect of Mg addition *Int. J. Hydrog. Energy* **33** 3489–92

Wang C, Dou B, Chen H, Song Y, Xu Y, Du X, Zhang L, Luo T and Tan C 2013 Renewable hydrogen production from steam reforming of glycerol by Ni–Cu–Al, Ni–Cu–Mg, Ni–Mg catalysts *Int. J. Hydrog. Energy* **38** 3562–71

Wang K, Dou B, Jiang B, Song Y, Zhang C, Zhang Q, Chen H and Xu Y 2016a Renewable hydrogen production from chemical looping steam reforming of ethanol using xCeNi/SBA-15 oxygen carriers in a fixed-bed reactor *Int. J. Hydrog. Energy* **41** 12899–909

Wang K, Dou B, Jiang B, Zhang Q, Li M, Chen H and Xu Y 2016b Effect of support on hydrogen production from chemical looping steam reforming of ethanol over Ni-based oxygen carriers *Int. J. Hydrog. Energy* **41** 17334–47

Wang P, Means N, Shekhawat D, Berry D and Massoudi M 2015 Chemical-looping combustion and gasification of coals and oxygen carrier development: a brief review *Energies* **8** 10605–35

Wang W, Fan L and Wang G 2017 Study on chemical looping reforming of ethanol (CLRE) for hydrogen production using $NiMn_2O_4$ spinel as oxygen carrier *J. Energy Inst.* **90** 884–92

Wang X, Li M, Wang M, Wang H, Li S, Wang S and Ma X 2009 Thermodynamic analysis of glycerol dry reforming for hydrogen and synthesis gas production *Fuel* **88** 2148–53

Wang Y, Zheng Y, Wang Y, Li K, Wang Y, Jiang L, Zhu X, Wei Y and Wang H 2019 Syngas production modified by oxygen vacancies over CeO2-ZrO2-CuO oxygen carrier via chemical looping reforming of methane *Appl. Surf. Sci.* **481** 151–60

Wang Z, Zhu M, He T, Zhang J, Wu J, Tian H and Wu J 2018 Chemical looping reforming of toluene as a biomass tar model compound over two types of oxygen carriers: $2CuO\text{-}2NiO/Al_2O_3$ and $CaFe_2O_4$ *Fuel* **222** 375–84

Wassie S A, Gallucci F, Zaabout A, Cloete S, Amini S and van Sint Annaland M 2017 Hydrogen production with integrated CO_2 capture in a novel gas switching reforming reactor: proof-of-concept *Int. J. Hydrog. Energy* **42** 14367–79

Wei G *et al* 2019 Chemical looping reforming of biomass based pyrolysis gas coupling with chemical looping hydrogen by using Fe/Ni/Al oxygen carriers derived from LDH precursors *Energy Convers. Manage.* **179** 304–13

Wei Y, Wang H, He F, Ao X and Zhang C 2007 CeO_2 as the oxygen carrier for partial oxidation of methane to synthesis gas in molten salts: thermodynamic analysis and experimental investigation *J. Nat. Gas Chem.* **16** 6–11

Wu G, Zhang C, Li S, Han Z, Wang T, Ma X and Gong J 2013 Hydrogen production via glycerol steam reforming over Ni/Al_2O_3: influence of nickel precursors *ACS Sustain. Chem. Eng.* **1** 1052–62

Yahom A, Powell J, Pavarajarn V, Onbhuddha P, Charojrochkul S and Assabumrungrat S 2014 Simulation and thermodynamic analysis of chemical looping reforming and CO_2 enhanced chemical looping reforming *Chem. Eng. Res. Des.* **92** 2575–83

Yamaguchi D, Tang L, Wong L, Burke N, Trimm D, Nguyen K and Chiang K 2011 Hydrogen production through methane–steam cyclic redox processes with iron-based metal oxides *Int. J. Hydrog. Energy* **36** 6646–56

Yan Y, Xu L, Wang L, Fu K, Tang M, Fan M and Ma X 2018 Syngas production from chemical-looping reforming of methane using iron-doped cerium oxides *Energy Technol.* **6** 1610–7

Yang G, Yu H, Peng F, Wang H, Yang J and Xie D 2011 Thermodynamic analysis of hydrogen generation via oxidative steam reforming of glycerol *Renew. Energy* **36** 2120–7

Yin X, Shen L, Wang S, Wang B and Shen C 2022 Double adjustment of Co and Sr in LaMnO3+δ perovskite oxygen carriers for chemical looping steam methane reforming *Appl. Catal.* B **301** 120816

Yu Z, Yang Y, Yang S, Zhang Q, Zhao J, Fang Y, Hao X and Guan G 2019 Iron-based oxygen carriers in chemical looping conversions: a review *Carbon Resour. Convers.* **2** 23–34

Yuan J, Zhao Y, Xu H, Lu C, Yang K, Zhu X and Li K 2020 Layered Mg-Al spinel supported Ce-Fe-Zr-O oxygen carriers for chemical looping reforming *Chin. J. Chem. Eng.* **28** 2668–76

Zafar Q, Mattisson T and Gevert B 2005 Integrated hydrogen and power production with CO_2 capture using chemical-looping reforming-redox reactivity of particles of CuO, Mn_2O_3, NiO, and Fe_2O_3 using SiO_2 as a support *Ind. Eng. Chem. Res.* **44** 3485–96

Zhang Q, Jiang B, Li L, Liu K, He N, Ma J, Zhang X and Tang D 2021a Multifunctional Ni-based oxygen carrier for H2 production by sorption enhanced chemical looping reforming of ethanol *Fuel Process. Technol.* **221** 106953

Zhang Q, Li L, Jiang B, Wang K, Tang D and Dou B 2017 An intelligent oxygen carrier of La2−xSrxNiO4−λ for hydrogen production by chemical looping reforming of ethanol *Int. J. Hydrog. Energy* **42** 17102–11

Zhang X, Su Y, Pei C, Zhao Z-J, Liu R and Gong J 2020 Chemical looping steam reforming of methane over Ce-doped perovskites *Chem. Eng. Sci.* **223** 115707

Zhang Y-K, Zhao Y-J, Yi Q, Wei G-Q, Shi L-J and Zhou H 2021b NiO/κ-CeZrO4 functional oxygen carriers with Niδ+ and oxygen vacancy synergy for chemical looping partial oxidation reforming of methane *Fuel Process. Technol.* **219** 106875

Zhao H, Guo L and Zou X 2015 Chemical-looping auto-thermal reforming of biomass using Cu-based oxygen carrier *Appl. Energy* **157** 408–15

Zhao K, Chen J, Li H, Zheng A and He F 2019 Effects of Co-substitution on the reactivity of double perovskite oxides $LaSrFe_{2-x}Co_xO_6$ for the chemical-looping steam methane reforming *J. Energy Inst.* **92** 594–603

Zhao K, He F, Huang Z, Wei G, Zheng A, Li H and Zhao Z 2016 Perovskite-type oxides $LaFe_{1-x}Co_xO_3$ for chemical looping steam methane reforming to syngas and hydrogen co-production *Appl. Energy* **168** 193–203

Zheng X, Su Q, Mi W and Zhang P 2014 Effect of steam reforming on methane-fueled chemical looping combustion with Cu-based oxygen carrier *Int. J. Hydrog. Energy* **39** 9158–68

Zheng Y, Li K, Wang H, Tian D, Wang Y, Zhu X, Wei Y, Zheng M and Luo Y 2017 Designed oxygen carriers from macroporous $LaFeO_3$ supported CeO_2 for chemical-looping reforming of methane *Appl. Catal.* B **202** 51–63

Zheng Y, Li K, Wang H, Zhu X, Wei Y, Zheng M and Wang Y 2016 Enhanced activity of $CeO_2\text{-}ZrO_2$ solid solutions for chemical-looping reforming of methane via tuning the macroporous structure *Energy Fuels* **30** 638–47

Zhu L, He Y, Li L and Wu P 2018 Tech-economic assessment of second-generation CCS: chemical looping combustion *Energy* **144** 915–27

Zhu M, Song Y, Chen S, Li M, Zhang L and Xiang W 2019 Chemical looping dry reforming of methane with hydrogen generation on Fe_2O_3/Al_2O_3 oxygen carrier *Chem. Eng. J.* **368** 812–23

Zhu X, Li K, Wei Y, Wang H and Sun L 2014 Chemical-looping steam methane reforming over a $CeO_2\text{-}Fe_2O_3$ oxygen carrier: evolution of its structure and reducibility *Energy Fuels* **28** 754–60

Zhu X, Wang H, Wei Y, Li K and Cheng X 2011 Hydrogen and syngas production from two-step steam reforming of methane using CeO_2 as oxygen carrier *J. Nat. Gas Chem.* **20** 281–6

Zhu X, Wei Y, Wang H and Li K 2013 Ce–Fe oxygen carriers for chemical-looping steam methane reforming *Int. J. Hydrog. Energy* **38** 4492–501